

# Mathematical Theories of Bourdon Pressure Tubes and Bending of Curved Pipes.

By Masasuke Tueda.

## Second Report: Example of Numerical Calculations.

*Second report gives the formulae, process and results of numerical calculations, taking for example the "Case II", that is the bending of curved pipes with the circular cross-section.*

### I. Formulae of Numerical Calculations.

As an example of numerical calculations, we take the "Case II", that is the bending of curved pipes with circular cross-section, from a comparatively thick walled pipe to a very thin walled one.

In order to make the range of utilisation of the results as large as possible, all the values are given in dimensionless numbers; and, for that purpose, we now assign the following notations to the dimensionless values.

$$\alpha = \frac{R_1}{r_0}, \quad \beta = \frac{h}{R_1}. \quad (124)$$

$$\frac{T_1}{2hE} = \sigma_1, \quad \frac{T_2}{2hE} = \sigma_2, \quad \frac{N}{2hE} = t, \quad \frac{\tau_0}{E} = t_0. \quad (125)$$

$$\frac{G_1}{2hR_1E} = g_1, \quad \frac{G_2}{2hR_1E} = g_2, \quad \frac{M}{hR_1^2E} = \mathfrak{M}. \quad (126)$$

$$\frac{\eta}{R_1} = \eta_R, \quad \frac{\nu}{R_1} = \nu_R. \quad (127)$$

From the equations (40), (34) and (31) in the first report we get

$$n^2 = \lambda_1 \lambda_2 - \mu^2 = \frac{3(1-\mu^2)}{\beta^2} - \mu^2,$$

that is,  $n$  and  $\beta$  have one to one correspondency to each other, and neglecting, with sufficient accuracy,  $\mu^2$  compared to  $n^2$ ,

$$n^2 = \frac{3(1-\mu^2)}{\beta^2}, \quad \text{or} \quad \frac{1}{\beta^2} = \frac{n^2}{3(1-\mu^2)}. \quad (128)$$

Putting, for the sake of simplicity,

$$V_s + \frac{\omega_0 R_1 \cos \varphi}{r} \phi_0 = V_e + \omega_0 \frac{a \cos \varphi}{1 + a \sin \varphi} t_0, \quad \phi_0 \equiv \Psi, \quad (129)$$

the equations (108)<sub>II</sub>, (109)<sub>II</sub>, (110)<sub>II</sub>, (111), (112), (115) and (122) become as follow;

$$\sigma_1 = -\frac{1}{n^2} \frac{a \cos \varphi}{1 + a \sin \varphi} \Psi + \frac{\sin \varphi}{1 + a \sin \varphi} t_0, \quad (130)$$

$$\sigma_2 = -\frac{1}{n^2} \frac{d\Psi}{d\varphi}, \quad (131)$$

$$t = \frac{1}{n^2} \frac{a \sin \varphi}{1 + a \sin \varphi} \Psi + \frac{\cos \varphi}{1 + a \sin \varphi} t_0, \quad (132)$$

$$\left. \begin{aligned} \varepsilon_1 &= \sigma_1 - \mu \sigma_2, \\ \varepsilon_2 &= \sigma_2 - \mu \sigma_1, \end{aligned} \right\} \quad (133)$$

$$\left. \begin{aligned} g_1 &= -\frac{1}{n^2} \left\{ \frac{d\theta}{d\varphi} + \frac{\mu a \cos \varphi}{1 + a \sin \varphi} \theta \right. \\ &\quad \left. - \frac{\varepsilon_1}{1 + a \sin \varphi} + \frac{\mu a \sin \varphi}{1 + a \sin \varphi} \omega_0 \right\}, \\ g_2 &= -\frac{1}{n^2} \left\{ \mu \frac{d\theta}{d\varphi} + \frac{a \cos \varphi}{1 + a \sin \varphi} \theta \right. \\ &\quad \left. + \frac{\varepsilon_2}{1 + a \sin \varphi} + \frac{a \sin \varphi}{1 + a \sin \varphi} \omega_0 \right\}, \end{aligned} \right\} \quad (134)$$

$$\eta_R = \left( \frac{1}{a} + \sin \varphi \right) (\varepsilon_2 - \omega_0), \quad (135)$$

$$\nu_R = \int_{-\frac{\pi}{2}}^{\varphi} (\varepsilon_1 \sin \varphi + \theta \cos \varphi) d\varphi, \quad (136)$$

$$\mathfrak{M} = 4 \int_{-\frac{\pi}{2}}^{+\frac{\pi}{2}} (\sigma_2 - g_2) \sin \varphi d\varphi. \quad (137)$$

From the equations (13), (14), (18) and (19), meridional and equatorial stresses  $\sigma_\varphi$  and  $\sigma_\psi$  at any point in the wall are given by

$$\left. \begin{aligned} \sigma_\varphi &= \left( 1 + \frac{z}{R_2} \right) \frac{T_1}{2h} + \frac{3z}{2h^3} G_1, \\ \sigma_\psi &= \left( 1 + \frac{z}{R_1} \right) \frac{T_2}{2h} + \frac{3z}{2h^3} G_2. \end{aligned} \right\} \quad (138)$$

Now let

$\sigma'_\varphi, \sigma'_\psi$  be the values of  $\sigma_\varphi$  and  $\sigma_\psi$  at  $z = +h$ ,  
the inside surface of the pipe,  
 $\sigma_{\varphi 0}, \sigma_{\psi 0}$  be the values at  $z = 0$ ,  
the middle surface of the wall,  
 $\sigma''_\varphi, \sigma''_\psi$  be the values at  $z = -h$ ,  
the outside surface of the pipe,

and  $\tau_m$  be the mean shearing stress on the equatorial section; then

$$\left. \begin{aligned} \sigma'_\varphi &= \left( 1 + \frac{h}{R_2} \right) \frac{T_1}{2h} + \frac{3G_1}{2h^2}, \\ \sigma'_\psi &= \left( 1 + \frac{h}{R_1} \right) \frac{T_2}{2h} + \frac{3G_2}{2h^2}, \end{aligned} \right\} \quad (139)$$

$$\left. \begin{aligned} \sigma_{\varphi 0} &= \frac{T_1}{2h}, \\ \sigma_{\psi 0} &= \frac{T_2}{2h}, \end{aligned} \right\} \quad (140)$$

$$\left. \begin{aligned} \sigma_{\varphi}'' &= \left(1 - \frac{h}{R_2}\right) \frac{T_1}{2h} - \frac{3G_1}{2h^2}, \\ \sigma_{\psi}'' &= \left(1 - \frac{h}{R_1}\right) \frac{T_2}{2h} - \frac{3G_2}{2h^2}, \end{aligned} \right\} \quad (141)$$

$$\tau_m = \frac{N}{2h}, \quad (142)$$

or, with the dimensionless values,

$$\left. \begin{aligned} \frac{\sigma'_{\varphi}}{E} &= \left(1 + \frac{a\beta \sin \varphi}{1 + a \sin \varphi}\right) \sigma_1 + \frac{3}{\beta} g_1, \\ \frac{\sigma'_{\psi}}{E} &= (1 + \beta) \sigma_2 + \frac{3}{\beta} g_2, \end{aligned} \right\} \quad (143)$$

$$\left. \begin{aligned} \frac{\sigma_{\varphi 0}}{E} &= \sigma_1, \\ \frac{\sigma_{\psi 0}}{E} &= \sigma_2, \end{aligned} \right\} \quad (144)$$

$$\left. \begin{aligned} \frac{\sigma''_{\varphi}}{E} &= \left(1 - \frac{a\beta \sin \varphi}{1 + a \sin \varphi}\right) \sigma_1 - \frac{3}{\beta} g_1, \\ \frac{\sigma''_{\psi}}{E} &= (1 - \beta) \sigma_2 - \frac{3}{\beta} g_2, \end{aligned} \right\} \quad (145)$$

$$\frac{\tau_m}{E} = t. \quad (146)$$

The results of the calculations will be given with the following magnitude, in order to be utilised conveniently, that is, for stresses

$$\frac{R_1^3}{M} \sigma'_{\varphi} = \frac{\sigma'_{\varphi}}{\beta E M}, \quad \frac{R_1^3}{M} \sigma'_{\psi} = \frac{\sigma'_{\psi}}{\beta E M}, \text{ etc., etc., (147)}_a$$

and for the deformations and displacements

$$\left. \begin{aligned} \frac{R_1^4 E}{M} \omega_1 &= \frac{a \omega_0}{\beta M}, \quad \frac{R_1^4 E}{M} \frac{\delta}{r_0} = \frac{a}{\beta M} (\eta_R)_{\varphi=0}, \\ \frac{R_1^2 E}{M} (\eta - \delta) &= \frac{\eta_R - (\eta_R)_{\varphi=0}}{\beta M}, \quad \frac{R_1^2 E}{M} \nu = \frac{\nu_R}{\beta M}, \end{aligned} \right\} \quad (147)_b$$

$$\text{where } \omega_1 = \frac{\omega}{r_0 \varphi} = \frac{\omega_0}{r_0} \quad (148)$$

is the value of  $\omega$  per unit length of the pipe.

## II. Process of Numerical Calculations.

### (A) Complementary Functions of the General Solution.

Complementary functions of the general solution are composed of eight infinite series shown in the equations (102) and (103), among which  $\theta_{1,1}$ ,  $\theta_{1,2}$ ,  $V_{1,1}$  and  $V_{1,2}$  need not to be calculated for the circular cross-section due to the equations (119), (104) and (105), and, therefore, we are to obtain only the second integrals of the complementary functions in the present case. These second integrals must be determined separately in two ranges, namely

$$\text{Range (I): } -\frac{\pi}{2} \leq \varphi \leq 0,$$

$$\text{and Range (II): } 0 \leq \varphi \leq +\frac{\pi}{2};$$

and, if necessary, we make distinction between them by adding the index I and II to each notation, respectively, and, otherwise, all the notations are recognized to be available in both ranges.

First of all, we assume certain numerical values to  $a$  and  $\beta$ , or  $a$  and  $n$ , then the equations (56) and (76) give  $\beta_q^*(q=0, 1, 2)$  to each ranges of  $\varphi$  separately, and then the coefficients of the series  $C_v^*$ , accordingly  $k_v^*$  and  $j_v^*$ , are obtained one after another by the equation (58) as many as necessary. With these coefficients, series  $\theta_{1,3}$ ,  $\theta_{1,4}$ ,  $V_{1,3}$  and  $V_{1,4}$  can be determined up to the desired term.

For instance, assuming  $a = \frac{1}{5}$  and  $n = 20$  or  $\beta = \frac{1}{12.106} \approx \frac{1}{12}$ , the first sixteen coefficients of the series are determined as shown in Table I. The value of  $\mu$  is assumed as 0.3. In the present numerical calculations, it is far more convenient to assume any round number to  $n$  than  $\beta$ .

### (B) Particular Integral.

In order to get the series  $\theta_2$  and  $V_{2,0}$  in the particular integral, we must calculate the values of  $\delta_q^*(q=0, 1, 2, 3, 4)$  by the equations (81)<sub>II</sub>, (93) and (101). In the equations (81)<sub>II</sub>,

$$\lambda_2 h \tau_0 r_0 = \frac{3(1-\mu^2)}{2a\beta^2} t_0 = \frac{n^2}{2a} t_0, \quad (149)$$

and both  $t_0$  and  $\omega_0$  are yet unknown constants. Therefore,  $\delta_q^*$  or  $\delta_v^*$  in the equation (94), have to be determined in the form

$$\delta_v^* = h_{vw} \omega_0 + h_{vt} t_0 + i(h_{vv}^* \omega_0 + h_{vt}^* t_0), \quad (150)$$

where  $h_{vw}$ ,  $h_{vt}$ ,  $h_{vv}^*$  and  $h_{vt}^*$  can be calculated easily by  $a$  and  $n$  only. In the following we make a distinction between the coefficients of  $\omega_0$  and  $t_0$  by adding the suffix  $\omega$  and  $t$  respectively. Then the coefficients  $C_v^{**}$  can be given by the equation (94) in the following form:

$$\left. \begin{aligned} C_v^{**} &= k_{vw}^{**} \omega_0 + k_{vt}^{**} t_0 + i(j_{vw}^{**} \omega_0 + j_{vt}^{**} t_0), \\ i.e., \quad k_v^{**} &= k_{vw}^{**} \omega_0 + k_{vt}^{**} t_0, \\ j_v^{**} &= j_{vw}^{**} \omega_0 + j_{vt}^{**} t_0. \end{aligned} \right\} \quad (151)$$

The required series of the particular integral are thus determined as the following:

$$\left. \begin{aligned} \theta_2 &= \theta_{2w} \omega_0 + \theta_{2t} t_0, \\ V_{2,0} &= V_{2w} \omega_0 + V_{2t} t_0, \end{aligned} \right\} \quad (152)$$

where

$$\left. \begin{aligned} \theta_{2\omega} &= \cos \varphi \sum_{v=0}^{\infty} j_{vv}^{**} (\sin \varphi \mp 1)^v, \\ \theta_{2t} &= \cos \varphi \sum_{v=0}^{\infty} j_{vt}^{**} (\sin \varphi \mp 1)^v, \\ V_{2\omega} &= \cos \varphi \sum_{v=0}^{\infty} (\mu j_{vv}^{**} - n k_{vv}^{**}) (\sin \varphi \mp 1)^v, \\ V_{2t} &= \cos \varphi \sum_{v=0}^{\infty} (\mu j_{vt}^{**} - n k_{vt}^{**}) (\sin \varphi \mp 1)^v. \end{aligned} \right\} \quad (153)$$

In the case of  $\alpha = \frac{1}{5}$  and  $\beta \approx \frac{1}{12}$ , for example, the coefficients of the above series become as shown in Table 2.

In the theory of ring shell by Wissler, the coefficients themselves of the infinite series in the particular integral shows no tendency to converge, moreover, the solution has a singular point at  $\varphi = 0$ , and, consequently, another series must be employed for the part near  $\varphi = 0$ . Table 2 indicates clearly great improvement in these points.

Table 1.

v	$+\frac{\pi}{2} \geq \varphi \geq 0$				$0 \geq \varphi \geq -\frac{\pi}{2}$			
	$k_v^*$	$j_v^*$	$\mu j_v^* + \mu k_v^*$	$\mu j_v^* - n k_v^*$	$k_v^*$	$j_v^*$	$\mu j_v^* + \mu k_v^*$	$\mu j_v^* - n k_v^*$
0	+1.	0.	+ 0.3	- 20.	+1.	0.	+ 0.3	- 20.
1	-0.38889	-1.11111	-22.3389	+ 7.4444	+0.25	-1.66667	-33.2583	- 5.5
2	-0.20370	+0.35185	+ 6.9759	+ 4.1796	-0.70833	-0.04167	- 1.0458	+14.1562
3	+0.00941	-0.04865	- 0.9701	- 0.2027	+0.22470	+0.08879	+ 1.8432	- 4.4674
4	+0.03339	+0.02634	+ 0.5369	- 0.6599	+0.01281	-0.10652	- 2.1266	- 0.2881
5	-0.02168	-0.01508	- 0.3081	+ 0.4291	+0.00759	+0.00024	+ 0.0071	- 0.1518
6	+0.01144	+0.00688	+ 0.1411	- 0.2266	+0.00951	-0.01001	- 0.1973	- 0.1932
7	-0.00581	-0.00288	- 0.0592	+ 0.1153	+0.00274	-0.00248	- 0.0487	- 0.0555
8	+0.00290	+0.00117	+ 0.0242	- 0.0577	+0.00193	-0.00143	- 0.0280	- 0.0390
9	-0.00143	-0.00047	- 0.0098	+ 0.0285	+0.00080	-0.00059	- 0.0115	- 0.0162
10	+0.00070	+0.00019	+ 0.0039	- 0.0140	+0.00043	-0.00027	- 0.0054	- 0.0086
11	-0.00034	-0.00007	- 0.0016	+ 0.0068	+0.00020	-0.00012	- 0.0024	- 0.0040
12	+0.00017	+0.00003	+ 0.0006	- 0.0033	+0.00010	-0.00006	- 0.0011	- 0.0020
13	-0.00008	-0.00001	- 0.0003	+ 0.0016	+0.00005	-0.00003	- 0.0005	- 0.0010
14	+0.00004		+ 0.0001	- 0.0008	+0.00002	-0.00001	- 0.0002	- 0.0005
15	-0.00002			+ 0.0004	+0.00001	-0.00001	- 0.0001	- 0.0002

Table 2.

v	$+\frac{\pi}{2} \geq \varphi \geq 0$				$0 \geq \varphi \geq -\frac{\pi}{2}$			
	$j_{vv}^{**}$	$j_{vt}^{**}$	$\mu j_{vv}^{**} - n k_{vv}^{**}$	$\mu j_{vt}^{**} - n k_{vt}^{**}$	$j_{vv}^{**}$	$j_{vt}^{**}$	$\mu j_{vv}^{**} - n k_{vv}^{**}$	$\mu j_{vt}^{**} - n k_{vt}^{**}$
0	0.	0.	0.	0.	0.	0.	0.	0.
1	+0.03296	+111.111	+21.4937	+ 51.85	-0.04944	-166.667	-34.1763	- 8.33
2	+0.34158	- 55.247	-10.9807	- 761.94	-0.86640	- 40.625	- 7.8765	+1661.77
3	-0.10600	+ 19.489	+ 3.8920	+235.48	+0.09559	- 3.621	- 0.6798	- 179.20
4	+0.00927	- 10.534	- 2.0773	- 28.46	-0.00321	- 16.859	- 3.4237	- 7.23
5	+0.00654	+ 5.658	+ 1.1097	- 8.15	-0.00274	- 3.754	- 0.7435	+ 2.98
6	-0.00664	- 2.809	- 0.5496	+ 10.95	+0.00719	- 2.562	- 0.5165	- 16.04
7	+0.00452	+ 1.343	+ 0.2623	- 7.97	+0.00213	- 1.052	- 0.2108	- 4.99
8	-0.00269	- 0.632	- 0.1233	+ 4.90	+0.00183	- 0.510	- 0.1025	- 3.99
9	+0.00149	+ 0.295	+ 0.0577	- 2.77	+0.00084	- 0.236	- 0.0475	- 1.84
10	-0.00080	- 0.138	- 0.0270	+ 1.50	+0.00047	- 0.111	- 0.0224	- 1.02
11	+0.00041	+ 0.065	+ 0.0127	- 0.78	+0.00023	- 0.053	- 0.0106	- 0.50
12	-0.00021	- 0.030	- 0.0060	+ 0.40	+0.00012	- 0.025	- 0.0050	- 0.26
13	+0.00011	+ 0.014	+ 0.0028	- 0.20	+0.00006	- 0.012	- 0.0024	- 0.13
14	-0.00005	- 0.007	- 0.0013	+ 0.10	+0.00003	- 0.006	- 0.0011	- 0.06
15	+0.00003	+ 0.003	+ 0.0006	- 0.05	+0.00002	- 0.003	- 0.0006	- 0.03

## (C) Boundary Conditions—I.

Since all the necessary series are obtained separately for each range of  $\varphi$  in the above, we must determine the integration constants  $B_3$  and  $B_4$  for both ranges to satisfy the boundary conditions at  $\varphi=0$ , that is the first four conditions of (121). The values of these series at  $\varphi=0$  are given by

$$\left. \begin{aligned} (\theta_{1,3})_0 &= \sum_{v=0}^{\infty} k_v^*(\mp 1)^v, \\ (\theta_{1,4})_0 &= \sum_{v=0}^{\infty} j_v^*(\mp 1)^v, \\ (V_{1,3})_0 &= \sum_{v=0}^{\infty} (n j_v^* + \mu k_v^*)(\mp 1)^v, \\ (V_{1,4})_0 &= \sum_{v=0}^{\infty} (\mu j_v^* - n k_v^*)(\mp 1)^v, \\ (\theta_{2w})_0 &= \sum_{v=0}^{\infty} j_{vw}^{**}(\mp 1)^v, \\ (\theta_{2t})_0 &= \sum_{v=0}^{\infty} j_{vt}^{**}(\mp 1)^v, \\ (V_{2w})_0 &= \sum_{v=0}^{\infty} (\mu j_{vw}^{**} - n k_{vw}^{**})(\mp 1)^v, \\ (V_{2t})_0 &= \sum_{v=0}^{\infty} (\mu j_{vt}^{**} - n k_{vt}^{**})(\mp 1)^v, \\ \left( \frac{d\theta_{1,3}}{d\varphi} \right)_0 &= \sum_{v=1}^{\infty} v k_v^*(\mp 1)^{v-1}, \\ \left( \frac{d\theta_{1,4}}{d\varphi} \right)_0 &= \sum_{v=1}^{\infty} v j_v^*(\mp 1)^{v-1}, \\ \left( \frac{dV_{1,3}}{d\varphi} \right)_0 &= \sum_{v=1}^{\infty} v(n j_v^* + \mu k_v^*)(\mp 1)^{v-1}, \\ \left( \frac{dV_{1,4}}{d\varphi} \right)_0 &= \sum_{v=1}^{\infty} v(\mu j_v^* - n k_v^*)(\mp 1)^{v-1}, \\ \left( \frac{d\theta_{2w}}{d\varphi} \right)_0 &= \sum_{v=1}^{\infty} v j_{vw}^{**}(\mp 1)^{v-1}, \\ \left( \frac{d\theta_{2t}}{d\varphi} \right)_0 &= \sum_{v=1}^{\infty} v j_{vt}^{**}(\mp 1)^{v-1}, \\ \left( \frac{dV_{2w}}{d\varphi} \right)_0 &= \sum_{v=1}^{\infty} v(\mu j_{vw}^{**} - n k_{vw}^{**})(\mp 1)^{v-1}, \\ \left( \frac{dV_{2t}}{d\varphi} \right)_0 &= \sum_{v=1}^{\infty} v(\mu j_{vt}^{**} - n k_{vt}^{**})(\mp 1)^{v-1}, \end{aligned} \right\} \quad (155)$$

where the upper sign of  $\mp$  corresponds to the range II, and the lower sign to the range I.

In the case of  $\alpha = \frac{1}{5}$  and  $\beta \approx \frac{1}{12}$ , for example, they become as shown in Table 3.

The four required boundary conditions are

then given in the following;

$$\left. \begin{aligned} B_3^I(\theta_{1,3})_0^I + B_4^I(\theta_{1,4})_0^I + \omega_0(\theta_{2w})_0^I + t_0(\theta_{2t})_0^I \\ = B_3^{II}(\theta_{1,3})_0^{II} + B_4^{II}(\theta_{1,4})_0^{II} + \omega_0(\theta_{2w})_0^{II} + t_0(\theta_{2t})_0^{II}, \\ B_3^I(V_{1,3})_0^I + B_4^I(V_{1,4})_0^I + \omega_0(V_{2w})_0^I + t_0(V_{2t})_0^I \\ = B_3^{II}(V_{1,3})_0^{II} + B_4^{II}(V_{1,4})_0^{II} + \omega_0(V_{2w})_0^{II} + t_0(V_{2t})_0^{II}, \\ B_3^I \left( \frac{d\theta_{1,3}}{d\varphi} \right)_0^I + B_4^I \left( \frac{d\theta_{1,4}}{d\varphi} \right)_0^I + \omega_0 \left( \frac{d\theta_{2w}}{d\varphi} \right)_0^I \\ + t_0 \left( \frac{d\theta_{2t}}{d\varphi} \right)_0^I = B_3^{II} \left( \frac{d\theta_{1,3}}{d\varphi} \right)_0^{II} + B_4^{II} \left( \frac{d\theta_{1,4}}{d\varphi} \right)_0^{II} \\ + \omega_0 \left( \frac{d\theta_{2w}}{d\varphi} \right)_0^{II} + t_0 \left( \frac{d\theta_{2t}}{d\varphi} \right)_0^{II}, \\ B_3^I \left( \frac{dV_{1,3}}{d\varphi} \right)_0^I + B_4^I \left( \frac{dV_{1,4}}{d\varphi} \right)_0^I + \omega_0 \left( \frac{dV_{2w}}{d\varphi} \right)_0^I \\ + t_0 \left( \frac{dV_{2t}}{d\varphi} \right)_0^I = B_3^{II} \left( \frac{dV_{1,3}}{d\varphi} \right)_0^{II} + B_4^{II} \left( \frac{dV_{1,4}}{d\varphi} \right)_0^{II} \\ + \omega_0 \left( \frac{dV_{2w}}{d\varphi} \right)_0^{II} + t_0 \left( \frac{dV_{2t}}{d\varphi} \right)_0^{II}. \end{aligned} \right\} \quad (156)$$

Solving these four simultaneous equations, we can determine four integration constants  $B_3^I$ ,  $B_4^I$ ,  $B_3^{II}$  and  $B_4^{II}$  as follows;

$$\left. \begin{aligned} B_3^I &= B_{3w}^I \omega_0 + B_{3t}^I t_0, \\ B_4^I &= B_{4w}^I \omega_0 + B_{4t}^I t_0, \\ B_3^{II} &= B_{3w}^{II} \omega_0 + B_{3t}^{II} t_0, \\ B_4^{II} &= B_{4w}^{II} \omega_0 + B_{4t}^{II} t_0. \end{aligned} \right\} \quad (157)$$

Table 4 shows these constants for  $\alpha = \frac{1}{5}$  and  $\beta \approx \frac{1}{12}$ .

Table 3.

$+\frac{\pi}{2} \geq \varphi \geq 0$	$0 \geq \varphi \geq -\frac{\pi}{2}$
$(\theta_{1,3})_0^{II} = +1.25380$	$(\theta_{1,3})_0^I = +0.80257$
$(\theta_{1,4})_0^{II} = +1.56473$	$(\theta_{1,4})_0^I = -1.74083$
$(V_{1,3})_0^{II} = +31.6708$	$(V_{1,3})_0^I = -34.5758$
$(V_{1,4})_0^{II} = -24.6067$	$(V_{1,4})_0^I = -16.5736$
$(\theta_{2w})_0^{II} = +0.40036$	$(\theta_{2w})_0^I = -0.81326$
$(\theta_{2t})_0^{II} = -207.379$	$(\theta_{2t})_0^I = -236.099$
$(V_{2w})_0^{II} = -40.5973$	$(V_{2w})_0^I = -47.8197$
$(V_{2t})_0^{II} = -1039.91$	$(V_{2t})_0^I = +1441.09$
$\left( \frac{d\theta_{1,3}}{d\varphi} \right)_0^{II} = -0.35561$	$\left( \frac{d\theta_{1,3}}{d\varphi} \right)_0^I = -0.29555$
$\left( \frac{d\theta_{1,4}}{d\varphi} \right)_0^{II} = -2.21976$	$\left( \frac{d\theta_{1,4}}{d\varphi} \right)_0^I = -2.00809$
$\left( \frac{dV_{1,3}}{d\varphi} \right)_0^{II} = -44.5018$	$\left( \frac{dV_{1,3}}{d\varphi} \right)_0^I = -40.2504$
$\left( \frac{dV_{1,4}}{d\varphi} \right)_0^{II} = +6.44627$	$\left( \frac{dV_{1,4}}{d\varphi} \right)_0^I = +5.30854$
$\left( \frac{d\theta_{2w}}{d\varphi} \right)_0^{II} = -0.84806$	$\left( \frac{d\theta_{2w}}{d\varphi} \right)_0^I = -1.43135$
$\left( \frac{d\theta_{2t}}{d\varphi} \right)_0^{II} = +387.308$	$\left( \frac{d\theta_{2t}}{d\varphi} \right)_0^I = -376.243$
$\left( \frac{dV_{2w}}{d\varphi} \right)_0^{II} = +76.1836$	$\left( \frac{dV_{2w}}{d\varphi} \right)_0^I = -75.6675$
$\left( \frac{dV_{2t}}{d\varphi} \right)_0^{II} = +2135.60$	$\left( \frac{dV_{2t}}{d\varphi} \right)_0^I = +2561.58$

Table 4.

$+\frac{\pi}{2} \geq \varphi \geq 0$	$0 \geq \varphi \geq -\frac{\pi}{2}$
$B_{3w}^{II} = +1.53297$	$B_{3w}^I = -2.01950$
$B_{3t}^{II} = +157.430$	$B_{3t}^I = +133.405$
$B_{4w}^{II} = -1.50206$	$B_{4w}^I = -1.38217$
$B_{4t}^{II} = +151.484$	$B_{4t}^I = -204.542$

Thus the infinite series  $\theta$  and  $V_s$  in the equations (10) and (105) and their derivatives can be obtained as the following:

$$\left. \begin{aligned} \theta &= \theta_w \cdot \omega_0 + \theta_t \cdot t_0, \\ V_s &= V_{sw} \cdot \omega_0 + V_{st} \cdot t_0, \\ \frac{d\theta}{d\varphi} &= \frac{d\theta_w}{d\varphi} \cdot \omega_0 + \frac{d\theta_t}{d\varphi} \cdot t_0, \\ \frac{dV_s}{d\varphi} &= \frac{dV_{sw}}{d\varphi} \cdot \omega_0 + \frac{dV_{st}}{d\varphi} \cdot t_0; \end{aligned} \right\} \quad (158)$$

$$\left. \begin{aligned} \text{where } \theta_w &= \cos \varphi \sum_{v=0}^{\infty} a_{vw} (\sin \varphi \mp 1)^v, \\ \theta_t &= \cos \varphi \sum_{v=0}^{\infty} a_{vt} (\sin \varphi \mp 1)^v, \\ V_{sw} &= \cos \varphi \sum_{v=0}^{\infty} b_{vw} (\sin \varphi \mp 1)^v, \\ V_{st} &= \cos \varphi \sum_{v=0}^{\infty} b_{vt} (\sin \varphi \mp 1)^v, \\ \frac{d\theta_w}{d\varphi} &= \cos^2 \varphi \sum_{v=1}^{\infty} v a_{vw} (\sin \varphi \mp 1)^{v-1} \\ &\quad - \sin \varphi \sum_{v=0}^{\infty} a_{vw} (\sin \varphi \mp 1)^v, \\ \frac{d\theta_t}{d\varphi} &= \cos^2 \varphi \sum_{v=1}^{\infty} v a_{vt} (\sin \varphi \mp 1)^{v-1} \\ &\quad - \sin \varphi \sum_{v=0}^{\infty} a_{vt} (\sin \varphi \mp 1)^v, \end{aligned} \right\} \quad (159)$$

$$\left. \begin{aligned} \frac{dV_{sw}}{d\varphi} &= \cos^2 \varphi \sum_{v=1}^{\infty} v b_{vw} (\sin \varphi \mp 1)^{v-1} \\ &\quad - \sin \varphi \sum_{v=0}^{\infty} b_{vw} (\sin \varphi \mp 1)^v, \\ \frac{dV_{st}}{d\varphi} &= \cos^2 \varphi \sum_{v=1}^{\infty} v b_{vt} (\sin \varphi \mp 1)^{v-1} \\ &\quad - \sin \varphi \sum_{v=0}^{\infty} b_{vt} (\sin \varphi \mp 1)^v, \end{aligned} \right\} \quad (160)$$

$$\left. \begin{aligned} \text{and } a_{vw} &= B_{3w} k_v^* + B_{4w} j_v^* + j_{vw}^{**}, \\ a_{vt} &= B_{3t} k_v^* + B_{4t} j_v^* + j_{vt}^{**}, \\ b_{vw} &= B_{3w} (\mu j_v^* + \mu k_v^*) + B_{4w} (\mu j_v^* - \mu k_v^*) \\ &\quad + (\mu j_{vw}^{**} - \mu k_{vw}^{**}), \\ b_{vt} &= B_{3t} (\mu j_v^* + \mu k_v^*) + B_{4t} (\mu j_v^* - \mu k_v^*) \\ &\quad + (\mu j_{vt}^{**} - \mu k_{vt}^{**}). \end{aligned} \right\} \quad (161)$$

Coefficients  $a_{vw}$ ,  $a_{vt}$ ,  $b_{vw}$  and  $b_{vt}$  for the case of  $\alpha = \frac{1}{5}$  and  $\beta \approx \frac{1}{12}$  are given in Table 5, which shows further better convergency than do those in Table 1 and Table 2.

After determining the value of  $V_s$ , the value of  $\Psi$  can be given as

$$\Psi = \Psi_w \cdot \omega_0 + \Psi_t \cdot t_0, \quad (162)$$

$$\left. \begin{aligned} \text{where } \Psi_w &= V_{sw} + \frac{\alpha \cos \varphi}{1 + \alpha \sin \varphi} \Phi_0, \\ \Psi_t &= V_{st}. \end{aligned} \right\} \quad (163)$$

#### (D) Boundary Condition—2.

Next, in order to determine the ratio of  $t_0$  to  $\omega_0$  by the sixth condition of (121), we must operate the integration of the second equation of (115) by the numerical integration. We must, for that purpose, calculate the values of  $\theta_w$ ,  $\theta_t$ ,  $\Psi_w$ ,  $\Psi_t$  and

Table 5.

v	$+\frac{\pi}{2} \geq \varphi \geq 0$				$0 \geq \varphi \geq -\frac{\pi}{2}$			
	$a_{vw}$	$a_{vt}$	$b_{vw}$	$b_{vt}$	$a_{vw}$	$a_{vt}$	$b_{vw}$	$b_{vt}$
0	+1.53297	+157.430	+30.5011	-2982.45	-2.01950	+133.405	+27.0375	+4130.86
1	+1.10576	-118.428	-23.9331	-2337.25	+1.74930	+207.587	+40.5908	-3320.18
2	-0.49919	-34.016	-6.5649	+969.43	+0.62167	-126.597	-25.3279	-1372.87
3	-0.01851	+13.601	+2.7093	+52.04	-0.48092	+8.194	+1.7725	+980.46
4	+0.02089	-1.287	-0.2631	-43.91	+0.11816	+6.638	+1.2692	-232.00
5	-0.00405	-0.039	-0.0071	+8.35	-0.01841	-2.791	-0.5481	+34.97
6	+0.00055	+0.034	+0.0071	-1.17	+0.00181	+0.754	+0.1491	-2.84
7	-0.00007	-0.008	-0.0017	+0.17	+0.00002	-0.181	-0.0358	-0.15
8	+0.00001	+0.002	+0.0005	-0.03	-0.00009	+0.040	+0.0079	+0.26
9		-0.002	-0.0002	+0.01	+0.00003	-0.009	-0.0019	-0.05
10		+0.001			-0.00001	+0.002	+0.0003	+0.03
11						-0.001	-0.0001	+0.01
12							+0.0001	

their derivatives at each range of  $\varphi$  with suitable intervals as shown in Table 6, for example, for the case of  $\alpha = \frac{1}{5}$  and  $\beta \approx \frac{1}{12}$ .

The sixth equation of (121) can be written as

$$\int_{-\frac{\pi}{2}}^{+\frac{\pi}{2}} (\epsilon_1 \sin \varphi + \theta \cos \varphi) d\varphi = 0, \quad (164)$$

or, substituting equations (133), (131), (130) and (162) into  $\epsilon_1$  in the above,

$$\omega_0 \int_{-\frac{\pi}{2}}^{+\frac{\pi}{2}} \left\{ n^2 \theta_w \cos \varphi - \frac{\alpha \sin \varphi \cos \varphi}{1 + \alpha \sin \varphi} \Psi_w + \mu \sin \varphi \frac{d\Psi_w}{d\varphi} \right\} d\varphi = 0$$

$$+ t_0 \int_{-\frac{\pi}{2}}^{+\frac{\pi}{2}} \left\{ n^2 \theta_t \cos \varphi - \frac{\alpha \sin \varphi \cos \varphi}{1 + \alpha \sin \varphi} \Psi_t + \mu \sin \varphi \frac{d\Psi_t}{d\varphi} + \frac{n^2 \sin^2 \varphi}{1 + \alpha \sin \varphi} \right\} d\varphi = 0. \quad (165)$$

Calculating the two values under each integral sign, and then integrating them by the numerical integration, we can determine the ratio  $t_{0w}$  of  $t_0$  to  $\omega_0$ , that is

$$t_0 = t_{0w} \omega_0. \quad (166)$$

In the case of  $\alpha = \frac{1}{5}$  and  $\beta \approx \frac{1}{12}$ , equations (165) and (166) become

$$-2278.5 \omega_0 + 3992009 t_0 = 0,$$

and

$$t_{0w} = 0.0005708.$$

Table 6.

$\varphi$	$\theta_w$	$\theta_t$	$\Psi_w$	$\Psi_t$	$\frac{d\theta_w}{d\varphi}$	$\frac{d\theta_t}{d\varphi}$	$\frac{d\Psi_w}{d\varphi}$	$\frac{d\Psi_t}{d\varphi}$
-90°	0.	0.	0.	0.	-2.0195	+133.41	+26.944	+4130.9
-85°	-0.1754	+ 11.70	+ 2.362	+ 359.0	-1.9918	+135.25	+27.312	+4077.2
-80°	-0.3460	+ 23.71	+ 4.787	+ 708.5	-1.9092	+140.60	+28.377	+3916.8
-75°	-0.5071	+ 36.32	+ 7.332	+1039.5	-1.7725	+148.88	+30.026	+3650.9
-70°	-0.6539	+ 49.75	+ 10.039	+1342.7	-1.5837	+159.20	+32.078	+3282.5
-65°	-0.7821	+ 64.13	+ 12.936	+1609.6	-1.3461	+170.42	+34.304	+2817.2
-60°	-0.8876	+ 79.48	+ 16.024	+1831.8	-1.0645	+181.21	+36.442	+2263.5
-55°	-0.9668	+ 95.71	+ 19.285	+2002.4	-0.7459	+190.23	+38.218	+1633.9
-50°	-1.0169	+112.59	+ 22.677	+2115.3	-0.3992	+196.16	+39.373	+946.4
-45°	-1.0360	+129.82	+ 26.133	+2166.3	-0.0355	+197.88	+39.681	+219.2
-40°	-1.0230	+146.98	+ 29.572	+2153.2	+0.3325	+194.51	+38.969	-520.1
-35°	-0.9783	+163.60	+ 32.901	+2075.9	+0.6913	+185.51	+37.131	-1245.6
-30°	-0.9030	+179.29	+ 36.019	+1937.0	+1.0266	+170.74	+34.137	-1929.2
-25°	-0.8001	+193.30	+ 38.827	+1741.3	+1.3253	+150.40	+30.034	-2543.6
-20°	-0.6731	+205.30	+ 41.232	+1495.8	+1.5754	+125.10	+24.940	-3064.5
-15°	-0.5268	+214.96	+ 43.156	+1209.7	+1.7671	+95.72	+19.037	-3471.6
-10°	-0.3666	+221.92	+ 44.538	+ 893.6	+1.8939	+63.40	+12.550	-3750.1
-5°	-0.1983	+225.97	+ 45.336	+ 559.2	+1.9519	+29.41	+ 5.735	-3891.4
0°	-0.0279	+227.04	+ 45.537	+ 218.5	+1.9410	- 4.93	- 1.146	-3893.8
+5°	+0.1394	+225.14	+ 45.143	- 116.8	+1.8644	- 38.28	- 7.803	-3769.8
+10°	+0.2957	+220.42	+ 44.187	- 435.8	+1.7274	- 69.55	-14.040	-3522.3
+15°	+0.4386	+213.09	+ 42.712	- 728.4	+1.5379	- 97.79	-19.667	-3166.1
+20°	+0.5629	+203.46	+ 40.776	- 985.8	+1.3056	-122.27	-24.543	-2719.9
+25°	+0.6655	+191.88	+ 38.453	-1201.1	+1.0410	-142.53	-28.576	-2204.5
+30°	+0.7440	+178.72	+ 35.815	-1369.2	+0.7549	-158.37	-31.729	-1641.6
+35°	+0.7969	+164.36	+ 32.940	-1486.9	+0.4580	-169.85	-34.013	-1052.8
+40°	+0.8239	+149.19	+ 29.902	-1552.8	+0.1603	-177.23	-35.483	-458.2
+45°	+0.8251	+133.54	+ 26.768	-1567.2	-0.1296	-180.97	-36.230	+123.7
+50°	+0.8017	+117.69	+ 23.597	-1532.0	-0.4038	-181.67	-36.373	+677.1
+55°	+0.7553	+101.90	+ 20.434	-1450.3	-0.6562	-179.99	-36.046	+1188.4
+60°	+0.6880	+ 86.33	+ 17.315	-1326.0	-0.8820	-176.66	-35.392	+1648.4
+65°	+0.6022	+ 71.09	+ 14.262	-1164.3	-1.0774	-172.40	-34.553	+2047.3
+70°	+0.5009	+ 56.24	+ 11.286	- 970.6	-1.2398	-167.88	-33.662	+2379.8
+75°	+0.3869	+ 41.78	+ 8.385	- 751.0	-1.3674	-163.70	-32.838	+2641.9
+80°	+0.2633	+ 27.65	+ 5.550	- 511.9	-1.4592	-160.34	-32.176	+2830.6
+85°	+0.1333	+ 13.76	+ 2.762	- 259.2	-1.5145	-158.18	-31.749	+2944.4
+90°	0.	0.	0.	0.	-1.5330	-157.43	-31.602	+2982.5

Substituting the equation (166) in the equations (162) and the first of (158),  $\theta$ ,  $\Psi$  and their derivatives are given in ratio to a single unknown constant  $\omega_0$ , that is

$$\left. \begin{aligned} \theta_0 &\equiv \frac{\theta}{\omega_0} = \theta_\omega + t_{0\omega}\theta_t, \\ \Psi_0 &\equiv \frac{\Psi}{\omega_0} = \Psi_\omega + t_{0\omega}\Psi_t. \end{aligned} \right\} \quad (167)$$

Table 7 shows these values in the case of  $\alpha = \frac{1}{5}$  and  $\beta \approx \frac{1}{12}$ .

Table 7.

$\varphi$	$\theta_0$	$\Psi_0$	$\frac{d\theta_0}{d\varphi}$	$\frac{d\Psi_0}{d\varphi}$
-90°	0.	0.	-1.9434	+29.302
-85°	-0.1688	+ 2.567	-1.9146	+29.639
-80°	-0.3325	+ 5.192	-1.8290	+30.612
-75°	-0.4863	+ 7.925	-1.6876	+32.110
-70°	-0.6255	+ 10.806	-1.4929	+33.951
-65°	-0.7455	+ 13.854	-1.2488	+35.912
-60°	-0.8422	+ 17.070	-0.9611	+37.734
-55°	-0.9122	+ 20.428	-0.6373	+39.151
-50°	-0.9526	+ 23.884	-0.2872	+39.913
-45°	-0.9619	+ 27.369	+0.0775	+39.806
-40°	-0.9391	+ 30.801	+0.4436	+38.672
-35°	-0.8849	+ 34.086	+0.7971	+36.420
-30°	-0.8007	+ 37.125	+1.1241	+33.036
-25°	-0.6898	+ 39.821	+1.4111	+28.582
-20°	-0.5559	+ 42.086	+1.6468	+23.191
-15°	-0.4041	+ 43.847	+1.8218	+17.055
-10°	-0.2399	+ 45.048	+1.9301	+10.410
-5°	-0.0693	+ 45.656	+1.9687	+ 3.514
0°	+0.1017	+ 45.661	+1.9382	- 3.368
+5°	+0.2679	+ 45.077	+1.8425	- 9.954
+10°	+0.4215	+ 43.938	+1.6877	-16.050
+15°	+0.5602	+ 42.296	+1.4821	-21.474
+20°	+0.6790	+ 40.214	+1.2358	-26.095
+25°	+0.7750	+ 37.767	+0.9596	-29.834
+30°	+0.8460	+ 35.034	+0.6645	-32.666
+35°	+0.8907	+ 32.091	+0.3611	-34.614
+40°	+0.9090	+ 29.016	+0.0591	-35.744
+45°	+0.9014	+ 25.874	-0.2328	-36.160
+50°	+0.8689	+ 22.722	-0.5075	-35.986
+55°	+0.8135	+ 19.606	-0.7590	-35.368
+60°	+0.7372	+ 16.558	-0.9829	-34.452
+65°	+0.6428	+ 13.597	-1.1758	-33.385
+70°	+0.5330	+ 10.732	-1.3356	-32.304
+75°	+0.4107	+ 7.956	-1.4609	-31.330
+80°	+0.2790	+ 5.257	-1.5508	-30.560
+85°	+0.1411	+ 2.614	-1.6048	-30.069
+90°	0.	0.	-1.6228	-29.900

Employing these values of  $\theta_0$ ,  $\Psi_0$  and their derivatives, we can calculate  $\frac{\sigma_1}{\omega_0}$ ,  $\frac{\sigma_2}{\omega_0}$ ,  $\frac{t}{\omega_0}$ ,  $\frac{\varepsilon_1}{\omega_0}$ ,

$\frac{\varepsilon_2}{\omega_0}$ ,  $\frac{g_1}{\omega_0}$ ,  $\frac{g_2}{\omega_0}$ ,  $\frac{\eta_R}{\omega_0}$  and  $\frac{\nu_R}{\omega_0}$  by the equations (130)~(136); and, further,  $\frac{\sigma'_\varphi}{E\omega_0}$ ,  $\frac{\sigma''_{\varphi 0}}{E\omega_0}$ ,  $\frac{\sigma''_\varphi}{E\omega_0}$ ,  $\frac{\sigma'_\psi}{E\omega_0}$ ,  $\frac{\sigma''_\psi}{E\omega_0}$  by the equations (143)~(146).

## (E) Boundary Condition—3.

Lastly, substituting the values of  $\sigma_2$  and  $g_2$  into the equation (137), and operating the numerical integration, we can determine the ratio  $\omega_m$  of  $\omega_0$  to  $\mathfrak{M}$ , that is

$$\omega_0 = \omega_m \mathfrak{M}. \quad (168)$$

In the case of  $\alpha = \frac{1}{5}$  and  $\beta \approx \frac{1}{12}$ , for example,

$$0.6606 \omega_0 = \mathfrak{M},$$

$$\omega_m = 1.514.$$

Then, equations (147) give the required results of the calculations as follows;

$$\left. \begin{aligned} \frac{R_1^3}{M} \sigma'_\varphi &= \frac{\sigma'_\varphi}{\beta E \mathfrak{M}} = \frac{\sigma'_\varphi}{E \omega_0} \cdot \frac{\omega_m}{\beta}, \text{ etc., etc.,} \\ \frac{R_1^4 E}{M} \omega_1 &= \frac{a \omega_0}{\beta \mathfrak{M}} = a \cdot \frac{\omega_m}{\beta}, \\ \frac{R_1^3 E}{M} \frac{\delta}{r_0} &= \frac{a}{\beta \mathfrak{M}} (\eta_R)_{\varphi=0} = a \cdot \left( \frac{\eta_R}{\omega_0} \right)_{\varphi=0} \cdot \frac{\omega_m}{\beta}, \\ \frac{R_1^2 E}{M} (\eta - \delta) &= \frac{\eta_R - (\eta_R)_{\varphi=0}}{\beta \mathfrak{M}} = \left[ \frac{\eta_R}{\omega_0} - \left( \frac{\eta_R}{\omega_0} \right)_{\varphi=0} \right] \frac{\omega_m}{\beta}, \\ \frac{R_1^2 E}{M} \nu &= \frac{\nu_R}{\beta \mathfrak{M}} = \frac{\nu_R}{\omega_0} \cdot \frac{\omega_m}{\beta}. \end{aligned} \right\} \quad (169)$$

## (F) Formulae for Numerical Integrations.

In order to operate the numerical integrations, the following Simpson's rules are employed;

$$\left. \begin{aligned} \int y d\varphi &= \frac{3}{8} \Delta \varphi [y_0 + 3y_1 + 3y_2 + 2y_3 + 3y_4 \\ &\quad + 3y_5 + 2y_6 + \dots + 2y_{3n-3} \\ &\quad + 3y_{3n-2} + 3y_{3n-1} + y_{3n}], \\ \int y d\varphi &= \frac{1}{3} \Delta \varphi [y_0 + 4y_1 + y_2], \\ \int y d\varphi &= \frac{1}{2} \Delta \varphi [y_0 + y_1]. \end{aligned} \right\} \quad (170)$$

## III. Comparison with the Extreme Cases.

Similarly as Kármán and the other authors of the approximate theories of bending of curved pipes, we now consider the correction factor  $K$ , that is the ratio of  $\omega_1$  or  $\omega_0$  obtained above to those calculated by the ordinary theory of bending of straight rods  $\omega_1^*$  or  $\omega_0^*$ , i.e.,

$$\left. \begin{aligned} K &= \frac{\omega_0}{\omega_0^*} = \frac{\omega_1}{\omega_1^*}, \\ \text{or } \omega_0 &= K \omega_0^* \text{ and } \omega_1 = K \omega_1^*. \end{aligned} \right\} \quad (171)$$

Now,  $\omega_0^*$  and  $\omega_1^*$  are given by

$$\omega_0^* = \frac{Mr_0}{EI} = \frac{\mathfrak{M}}{2\pi a(1+\beta^2)}, \quad (172)$$

$$\omega_1^* = \frac{M}{EI} = \frac{\mathfrak{M}}{2\pi(1+\beta^2)} \frac{I}{R_1}, \quad (173)$$

$$\text{or } \frac{R_1^4 E}{M} \omega_1^* = \frac{I}{2\pi\beta(1+\beta^2)},$$

where  $I$  is the moment of inertia of the cross-section. Then we have

$$K = 2\pi a(1+\beta^2) \omega_m. \quad (174)$$

In the case of  $a=\frac{I}{5}$  and  $\beta \approx \frac{I}{12}$ ,  $K=1.915$ .

As an extreme case of the present problem, we can take the case  $\beta=1$ , that is the bending of solid curved rods. In this extreme case,

$$\left. \begin{aligned} \omega_0 &= \frac{M}{ExFr_0}, \\ \omega_1 &= \frac{M}{ExFr_0^2}, \end{aligned} \right\} \quad (175)$$

where  $x$  is a coefficient which depends on the shape of the cross-section, and  $F$  the cross-sectional area. Then

$$K = \frac{I}{xFr_0^2} = \frac{I}{1+2a^2+5a^4+\dots}, \quad (176)$$

$$\frac{R_1^4 E}{M} \omega_1 = \frac{I}{4\pi(1+2a^2+5a^4+\dots)}. \quad (177)$$

Another extreme case is  $a=0$ , the straight pipes, and in which,

$$\left. \begin{aligned} \frac{R_1^3}{M} \sigma_{\psi 0} &= \frac{I}{2\pi\beta(1+\beta^2)} \sin \varphi, \\ \frac{R_1^3}{M} \sigma'_{\psi} &= \frac{1-\beta}{2\pi\beta(1+\beta^2)} \sin \varphi, \\ \frac{R_1^3}{M} \sigma''_{\psi} &= \frac{1+\beta}{2\pi\beta(1+\beta^2)} \sin \varphi, \end{aligned} \right\} \quad (178)$$

$$\omega_1 = \omega_1^*. \quad (179)$$

#### IV. Results of Numerical Calculations.

The calculations are made in the following six cases :

$$\left. \begin{aligned} a &= \frac{I}{5}, \\ a &= \frac{I}{10}, \end{aligned} \right\} \left\{ \begin{array}{ll} n=10, & \beta = \frac{I}{6.055} \approx \frac{I}{6}, \\ n=20, & \beta = \frac{I}{12.106} \approx \frac{I}{12}, \\ n=100, & \beta = \frac{I}{60.52} \approx \frac{I}{60}. \end{array} \right.$$

Results of the calculations are shown in Table 8~Table 17 and Fig. 5~Fig. 21.

To prove the accuracy of inserting the approximation of  $\epsilon_1$  and  $\epsilon_2$  as equations (29),  $G_1$  and  $G_2$ , along with the terms of  $\epsilon_1$  and  $\epsilon_2$  in them, are given in the upper halves of Fig. 22~Fig. 25; for the case of  $\beta \approx \frac{I}{60}$ , both  $\epsilon_1$  and  $\epsilon_2$  become so small that they cannot be indicated clearly on the diagram. Lower halves of Fig. 22~Fig. 25 and also Fig. 26 shows the comparison between the accurate and the approximated values of  $\epsilon_1$  and  $\epsilon_2$ . From these diagrams, we can easily recognize, that, in the case of a very thin wall, both  $\epsilon_1$  and  $\epsilon_2$  may be neglected altogether, but, in the comparatively thick walled cases, to neglect of them will surely cause considerable error in the results, and also that the errors due to the approximation of the equations (29) are very trifling compared to the magnitudes of  $G_1$  and  $G_2$  themselves, even in the comparatively thick walled pipes.

To compare the results of the present theory with those of Kármán's first approximation, dotted curves are added in Fig. 5~Fig. 10.

Correction factors  $K$  by some approximate theories are given in Table 18.

#### V. Conclusions.

1. All the approximate theories only give  $\sigma_{\psi 0}$ ,  $(\gamma-\delta)$  and  $\omega$  alone, and the other kinds of stresses and displacements are obtained accurately for the first time in the present paper.

2. In the case of very thin walled curved pipes, so called bending stress  $\sigma_{\psi}$  becomes compressive at the extremity of the tension side, and similarly becomes tensile at the extremity of the compression side.

3. In the case of very thin walled curved pipes, the secondary bending stress  $\sigma_{\psi}$  becomes considerably greater than  $\sigma_{\psi 0}$ , therefore, the calculation of strength in such a case must be made with  $\sigma_{\psi}$  instead of  $\sigma_{\psi 0}$ .

4. So long as the correction factors  $K$  are concerned, Kármán's second approximate theory offers results sufficiently accurate for practice.

5. The values of  $K$  by the approximate theories are all dependent upon the ratio  $\beta/a$  only, which is now proved to be not satisfied accurately by the present theory.

Table 8.

$\varphi$	$\frac{R_1^3}{M}\sigma_{\psi 0}$	$\frac{R_1^3}{M}\sigma'_{\psi}$	$\frac{R_1^3}{M}\sigma''_{\psi}$	$\frac{R_1^3}{M}\sigma_{\varphi 0}$	$\frac{R_1^3}{M}\sigma'_{\varphi}$	$\frac{R_1^3}{M}\sigma''_{\varphi}$	$\frac{R_1^3}{M}\tau_m$	$\frac{R_1^2 E}{M}v$	$\frac{R_1^2 E}{M}(\eta - \delta)$
-90°	-0.9380	-0.3542	-1.5218	-0.0063	+0.9973	-1.0099	0.	0.	+1.4445
-75°	-0.9213	-0.3802	-1.4624	-0.0217	+0.8405	-0.8839	-0.0568	-0.0967	+1.2975
-60°	-0.8580	-0.4402	-1.2759	-0.0632	+0.4195	-0.5458	-0.0972	-0.3175	+0.9295
-45°	-0.7220	-0.4886	-0.9555	-0.1173	-0.1330	-0.1017	-0.1090	-0.6863	+0.5117
-30°	-0.5021	-0.4760	-0.5283	-0.1662	-0.6459	+0.3135	-0.0894	-1.0987	+0.2028
-15°	-0.2181	-0.3729	-0.0633	-0.1938	-0.9711	+0.5836	-0.0464	-1.3835	+0.0562
0°	+0.0849	-0.1826	+0.3525	-0.1923	-1.0332	+0.6486	+0.0051	-1.4085	0.
+15°	+0.3573	+0.0631	+0.6515	-0.1645	-0.8449	+0.5159	+0.0491	-1.1592	-0.1020
+30°	+0.5654	+0.3205	+0.8104	-0.1206	-0.4864	+0.2453	+0.0749	-0.7428	-0.3552
+45°	+0.7001	+0.5496	+0.8506	-0.0728	-0.0670	-0.0786	+0.0791	-0.3266	-0.7662
+60°	+0.7729	+0.7243	+0.8214	-0.0320	+0.3096	-0.3736	+0.0640	-0.0503	-1.2341
+75°	+0.8041	+0.8315	+0.7767	-0.0051	+0.5659	-0.5762	+0.0354	+0.0388	-1.6076
+90°	+0.8122	+0.8674	+0.7570	+0.0042	+0.6563	-0.6479	0.	0.	-1.7493

Table 9.

$\varphi$	$\frac{R_1^3}{M}\sigma_{\psi 0}$	$\frac{R_1^3}{M}\sigma'_{\psi}$	$\frac{R_1^3}{M}\sigma''_{\psi}$	$\frac{R_1^3}{M}\sigma_{\varphi 0}$	$\frac{R_1^3}{M}\sigma'_{\varphi}$	$\frac{R_1^3}{M}\sigma''_{\varphi}$	$\frac{R_1^3}{M}\tau_m$	$\frac{R_1^2 E}{M}v$	$\frac{R_1^2 E}{M}(\eta - \delta)$
-90°	-1.342	+0.086	-2.771	-0.013	+3.392	-3.419	0.	0.	+11.573
-75°	-1.471	-0.134	-2.808	-0.036	+2.956	-3.028	-0.084	-0.308	+10.411
-60°	-1.729	-0.687	-2.771	-0.106	+1.698	-1.909	-0.158	-1.688	+7.456
-45°	-1.824	-1.289	-2.359	-0.215	-0.145	-0.286	-0.198	-4.471	+4.007
-30°	-1.514	-1.616	-1.411	-0.333	-2.057	+1.391	-0.179	-7.931	+1.403
-15°	-0.781	-1.465	-0.098	-0.412	-3.393	+2.568	-0.099	-10.645	+0.225
0°	+0.154	-0.861	+1.169	-0.418	-3.698	+2.861	+0.011	-11.358	0.
+15°	+0.984	-0.023	+1.990	-0.353	-2.955	+2.248	+0.105	-9.766	-0.411
+30°	+1.497	+0.785	+2.208	-0.248	-1.526	+1.030	+0.154	-6.659	-1.922
+45°	+1.657	+1.382	+1.931	-0.140	+0.078	-0.358	+0.153	-3.379	-4.663
+60°	+1.578	+1.726	+1.431	-0.057	+1.433	-1.547	+0.117	-1.052	-7.911
+75°	+1.435	+1.875	+0.996	-0.007	+2.302	-2.317	+0.061	-0.066	-10.524
+90°	+1.370	+1.913	+0.827	+0.009	+2.598	-2.580	0.	0.	-11.522

Table 10.

$\varphi$	$\frac{R_1^3}{M}\sigma_{\psi 0}$	$\frac{R_1^3}{M}\sigma'_{\psi}$	$\frac{R_1^3}{M}\sigma''_{\psi}$	$\frac{R_1^3}{M}\sigma_{\varphi 0}$	$\frac{R_1^3}{M}\sigma'_{\varphi}$	$\frac{R_1^3}{M}\sigma''_{\varphi}$	$\frac{R_1^3}{M}\tau_m$	$\frac{R_1^2 E}{M}v$	$\frac{R_1^2 E}{M}(\eta - \delta)$
-90°	+ 3.43	+ 8.55	- 1.68	- 0.00	+ 10.47	- 10.47	0.	0.	+485.6
-75°	+ 2.57	+ 9.27	- 4.13	+ 0.05	+ 15.48	- 15.38	+ 0.201	- 3.3	+465.7
-60°	- 3.01	+ 7.33	- 13.36	+ 0.11	+ 25.97	- 25.75	+ 0.197	- 34.5	+394.7
-45°	- 15.88	- 4.42	- 27.34	- 0.24	+ 25.85	- 26.32	- 0.232	- 139.3	+262.9
-30°	- 27.09	- 22.77	- 31.41	- 1.40	- 1.13	- 1.67	- 0.805	- 341.8	+110.9
-15°	- 21.40	- 30.37	- 12.43	- 2.87	- 42.49	+ 36.76	- 0.766	- 567.0	+ 17.3
0°	+ 0.99	- 16.29	+ 18.26	- 3.39	- 60.74	+ 53.96	+ 0.002	- 663.9	0.
+15°	+ 21.18	+ 7.36	+ 34.99	- 2.52	- 39.92	+ 34.88	+ 0.678	- 560.7	- 19.4
+30°	+ 24.59	+ 20.64	+ 28.55	- 1.15	- 3.39	+ 1.08	+ 0.669	- 343.0	- 113.8
+45°	+ 15.12	+ 18.40	+ 11.89	- 0.25	+ 19.38	- 19.87	+ 0.248	- 148.5	- 264.0
+60°	+ 4.35	+ 9.14	- 0.44	+ 0.04	+ 22.25	- 22.16	- 0.072	- 41.3	- 401.9
+75°	- 1.67	+ 1.81	- 5.14	+ 0.03	+ 16.44	- 16.37	- 0.117	- 4.9	- 485.5
+90°	- 3.31	- 0.69	- 5.93	+ 0.00	+ 13.19	- 13.19	0.	0.	- 511.8

Table 11.

$\varphi$	$\frac{R_1^3}{M} \sigma_{\psi 0}$	$\frac{R_1^3}{M} \sigma'_{\psi}$	$\frac{R_1^3}{M} \sigma''_{\psi}$	$\frac{R_1^3}{M} \sigma_{\varphi 0}$	$\frac{R_1^3}{M} \sigma'_{\varphi}$	$\frac{R_1^3}{M} \sigma''_{\varphi}$	$\frac{R_1^3}{M} \tau_m$	$\frac{R_1^2 E}{M} v$	$\frac{R_1^2 E}{M} (\eta - \delta)$
-90°	-0.9712	-0.6171	-1.3252	+0.0007	+0.5058	-0.5045	0.	0.	+0.5653
-75°	-0.9385	-0.6100	-1.2670	-0.0065	+0.4327	-0.4456	-0.0271	-0.0906	+0.5050
-60°	-0.8408	-0.5843	-1.0973	-0.0260	+0.2331	-0.2852	-0.0464	-0.2210	+0.3534
-45°	-0.6805	-0.5281	-0.8330	-0.0518	-0.0327	-0.0708	-0.0527	-0.4116	+0.1747
-30°	-0.4668	-0.4287	-0.5050	-0.0760	-0.2888	+0.1369	-0.0464	-0.6010	+0.0673
-15°	-0.2170	-0.2802	-0.1538	-0.0917	-0.4665	+0.2830	-0.0253	-0.7313	+0.0161
0°	+0.0451	-0.0889	+0.1792	-0.0951	-0.5234	+0.3333	-0.0006	-0.7198	0.
+15°	+0.2945	+0.1299	+0.4590	-0.0854	-0.4554	+0.2845	+0.0223	-0.5723	-0.0532
+30°	+0.5096	+0.3522	+0.6671	-0.0662	-0.2857	+0.1533	+0.0375	-0.3317	-0.1998
+45°	+0.6779	+0.5538	+0.8020	-0.0428	-0.0698	-0.0158	+0.0420	-0.1046	-0.4448
+60°	+0.7957	+0.7130	+0.8783	-0.0211	+0.1360	-0.1782	+0.0354	+0.0309	-0.7229
+75°	+0.8638	+0.8182	+0.9134	-0.0060	+0.2825	-0.2945	+0.0201	+0.0561	-0.9468
+90°	+0.8862	+0.8494	+0.9231	-0.0005	+0.3354	-0.3364	0.	0.	-1.0321

Table 12.

$\varphi$	$\frac{R_1^3}{M} \sigma_{\psi 0}$	$\frac{R_1^3}{M} \sigma'_{\psi}$	$\frac{R_1^3}{M} \sigma''_{\psi}$	$\frac{R_1^3}{M} \sigma_{\varphi 0}$	$\frac{R_1^3}{M} \sigma'_{\varphi}$	$\frac{R_1^3}{M} \sigma''_{\varphi}$	$\frac{R_1^3}{M} \tau_m$	$\frac{R_1^2 E}{M} v$	$\frac{R_1^2 E}{M} (\eta - \delta)$
-90°	-1.828	-1.040	-2.616	-0.003	+1.836	-1.842	0.	0.	+5.934
-75°	-1.803	-1.085	-2.521	-0.017	+1.582	-1.615	-0.050	-0.298	+5.323
-60°	-1.701	-1.187	-2.214	-0.054	+0.870	-0.977	-0.087	-1.037	+3.798
-45°	-1.471	-1.253	-1.688	-0.105	-0.102	-0.108	-0.101	-2.525	+2.022
-30°	-1.074	-1.179	-0.969	-0.156	-1.056	+0.745	-0.087	-4.265	+0.701
-15°	-0.529	-0.904	-0.155	-0.190	-1.719	+1.340	-0.048	-5.738	+0.110
0°	+0.087	-0.436	+0.610	-0.196	-1.912	+1.520	+0.003	-6.113	0.
+15°	+0.672	+0.152	+1.192	-0.175	-1.605	+1.255	+0.050	-5.302	-0.193
+30°	+1.138	+0.756	+1.520	-0.133	-0.916	+0.650	+0.080	-3.588	-1.008
+45°	+1.453	+1.288	+1.618	-0.083	-0.057	-0.109	+0.086	-1.771	-2.493
+60°	+1.614	+1.669	+1.560	-0.038	+0.744	-0.820	+0.071	-0.503	-4.434
+75°	+1.685	+1.909	+1.462	-0.008	+1.304	-1.320	+0.040	+0.036	-5.977
+90°	+1.703	+1.986	+1.419	+0.003	+1.502	-1.497	0.	0.	-6.813

Table 13.

$\varphi$	$\frac{R_1^3}{M} \sigma_{\psi 0}$	$\frac{R_1^3}{M} \sigma'_{\psi}$	$\frac{R_1^3}{M} \sigma''_{\psi}$	$\frac{R_1^3}{M} \sigma_{\varphi 0}$	$\frac{R_1^3}{M} \sigma'_{\varphi}$	$\frac{R_1^3}{M} \sigma''_{\varphi}$	$\frac{R_1^3}{M} \tau_m$	$\frac{R_1^2 E}{M} v$	$\frac{R_1^2 E}{M} (\eta - \delta)$
-90°	+ 0.77	+ 7.65	- 6.11	-0.00	+20.01	-20.01	0.	0.	+473.2
-75°	- 1.50	+ 5.55	- 8.56	-0.00	+20.24	-20.24	+0.001	- 9.5	+436.5
-60°	- 7.52	- 0.82	- 1.21	-0.06	+18.05	-18.18	-0.106	- 50.7	+334.3
-45°	-14.19	-10.11	-18.28	-0.31	+ 8.10	- 8.71	-0.303	-158.2	+196.4
-30°	-16.55	-17.88	-15.22	-0.74	-10.39	+ 8.90	-0.429	-313.7	+ 74.2
-15°	-11.04	-18.46	-3.62	-1.19	-29.19	+26.81	-0.315	-470.5	+ 11.0
0°	+ 0.35	-10.32	+11.02	-1.35	-36.83	+34.13	+0.003	-531.6	0.
+15°	+11.17	+ 2.11	+20.23	-1.16	-28.26	+25.95	+0.301	-469.1	- 12.1
+30°	+15.59	+11.38	+19.79	-0.67	-10.08	+ 8.74	+0.391	-312.7	- 78.7
+45°	+13.23	+14.05	+12.41	-0.28	+ 6.83	- 7.40	+0.282	-154.5	-199.9
+60°	+ 7.44	+11.34	+ 3.53	-0.07	+16.40	-16.51	+0.122	- 49.7	-336.9
+75°	+ 2.37	+ 7.31	- 2.57	-0.01	+19.12	-19.13	+0.026	- 5.7	-439.2
+90°	+ 0.45	+ 5.70	- 4.81	+0.00	+19.89	-19.89	0.	0.	-476.5

Table 14.

		$\alpha = \frac{R_1}{r_0} = 0$ , (Straight pipe)					
$\varphi$	$\beta = \frac{h}{R_1} \approx \frac{1}{6}$	$\beta = \frac{h}{R_1} \approx \frac{1}{12}$			$\beta = \frac{h}{R_1} \approx \frac{1}{60}$		
		$\frac{R_1^3}{M} \sigma_{\psi 0}$	$\frac{R_1^3}{M} \sigma'_{\psi}$	$\frac{R_1^3}{M} \sigma''_{\psi}$	$\frac{R_1^3}{M} \sigma_{\psi 0}$	$\frac{R_1^3}{M} \sigma'_{\psi}$	$\frac{R_1^3}{M} \sigma''_{\psi}$
$0^\circ$	0.	0.	0.	0.	0.	0.	0.
$\pm 15^\circ$	$\pm 0.2428$	$\pm 0.2027$	$\pm 0.2829$	$\pm 0.495$	$\pm 0.454$	$\pm 0.536$	$\pm 2.492$
$\pm 30^\circ$	$\pm 0.4691$	$\pm 0.3916$	$\pm 0.5466$	$\pm 0.957$	$\pm 0.878$	$\pm 1.036$	$\pm 4.815$
$\pm 45^\circ$	$\pm 0.6633$	$\pm 0.5538$	$\pm 0.7728$	$\pm 1.353$	$\pm 1.241$	$\pm 1.465$	$\pm 6.809$
$\pm 60^\circ$	$\pm 0.8124$	$\pm 0.6782$	$\pm 0.9466$	$\pm 1.657$	$\pm 1.520$	$\pm 1.794$	$\pm 8.340$
$\pm 75^\circ$	$\pm 0.9061$	$\pm 0.7565$	$\pm 1.0557$	$\pm 1.849$	$\pm 1.696$	$\pm 2.001$	$\pm 9.302$
$\pm 90^\circ$	$\pm 0.9381$	$\pm 0.7832$	$\pm 1.0930$	$\pm 1.914$	$\pm 1.756$	$\pm 2.072$	$\pm 9.630$

Table 15.

		Value of $-\frac{R_1^3 E}{M} \frac{\delta}{r_0}$		
$\alpha \setminus \beta$		$\frac{1}{6}$	$\frac{1}{12}$	$\frac{1}{60}$
$\frac{1}{5}$	5.759	18.05	479.9	
$\frac{1}{10}$	9.966	23.69	520.4	

Table 16.

		Value of $\frac{R_1^4 E}{M} \omega_1$			
$\alpha \setminus \beta$		$\frac{1}{6}$	$\frac{1}{12}$	$\frac{1}{60}$	
$\frac{1}{5}$	0.07321	1.180	3.665	98.37	
$\frac{1}{10}$	0.07799	1.004	2.384	47.38	
0	0.07958	0.938	1.914	9.63	

Table 17.

		Value of $K$			
$\alpha \setminus \beta$		$\frac{1}{6}$	$\frac{1}{12}$	$\frac{1}{60}$	
$\frac{1}{5}$	0.92	1.263	1.915	10.008	
$\frac{1}{10}$	0.98	1.075	1.245	4.921	
0	1.	1.	1.	1.	

Table 18.

Value of $K$ calculated by approximate theories.						
$\alpha = \frac{R_1}{r_0} =$	$\frac{1}{5}$			$\frac{1}{10}$		
$\beta = \frac{h}{R_1} \approx$	$\frac{1}{6}$	$\frac{1}{12}$	$\frac{1}{60}$	$\frac{1}{6}$	$\frac{1}{12}$	$\frac{1}{60}$
Kármán. (1st. approximation)	1.267	1.980	7.779	1.068	1.267	4.859
Matumura.						
Kármán. (2nd. approximation)	1.267	1.983	10.443	1.068	1.267	5.169
Hovgaard.	1.153	1.801	7.079	0.972	1.153	4.422
Lorenz.	1.275	2.099	28.473	1.069	1.275	7.868

Fig. 5.

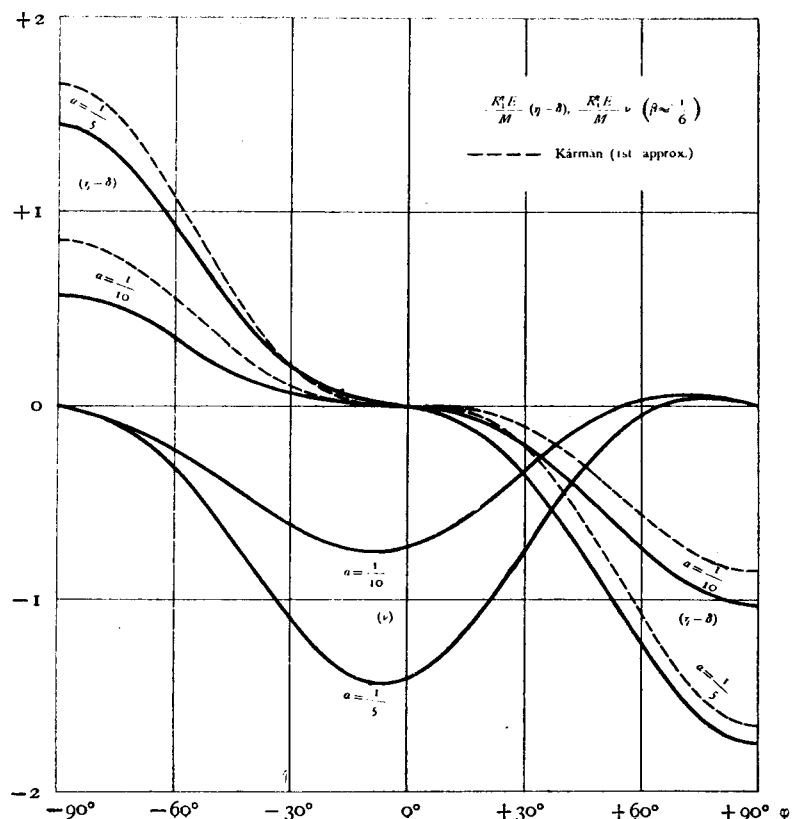


Fig. 6.

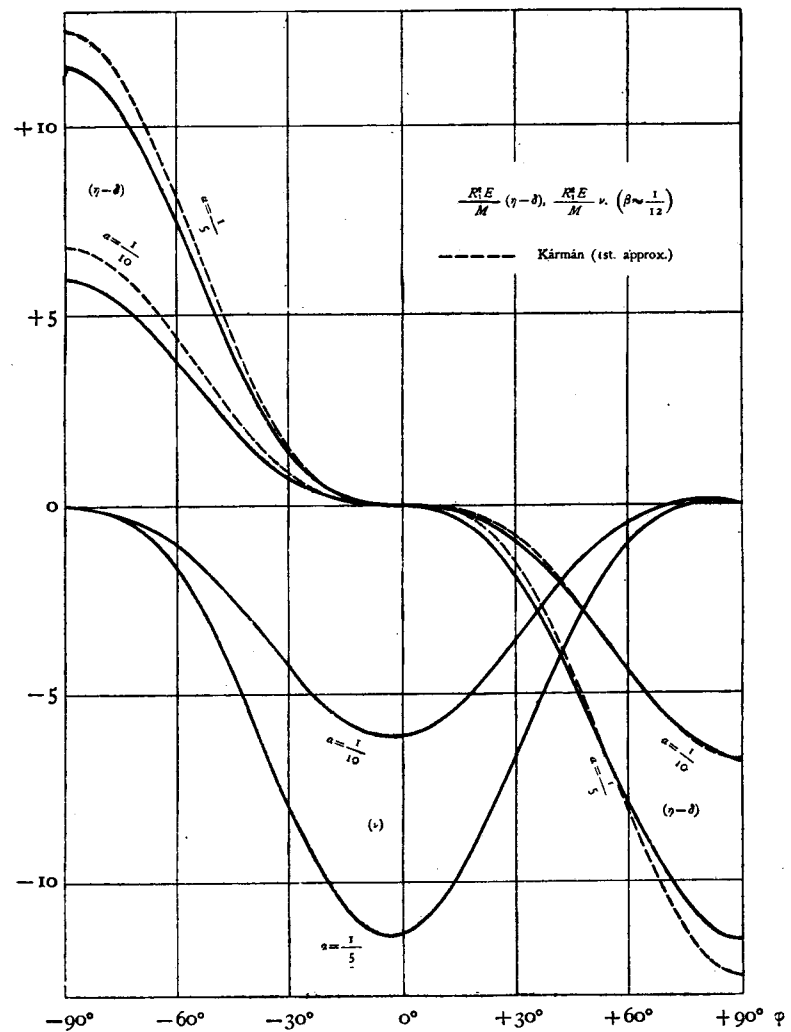


Fig. 7.

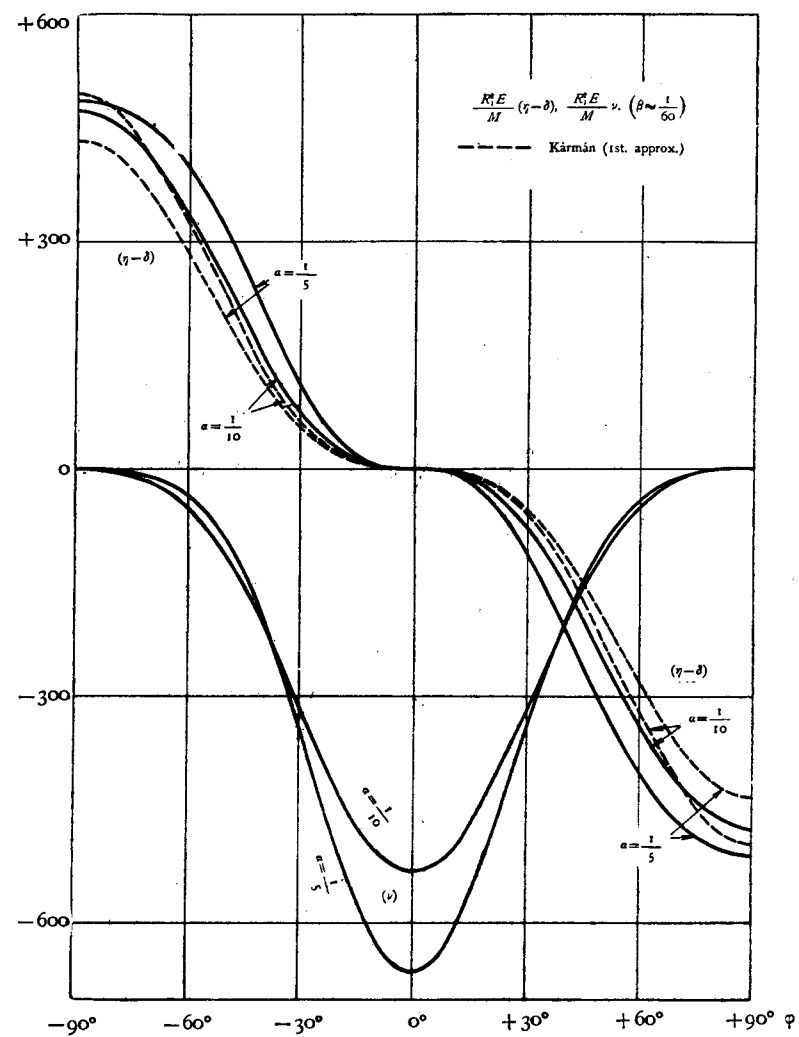


Fig. 8.

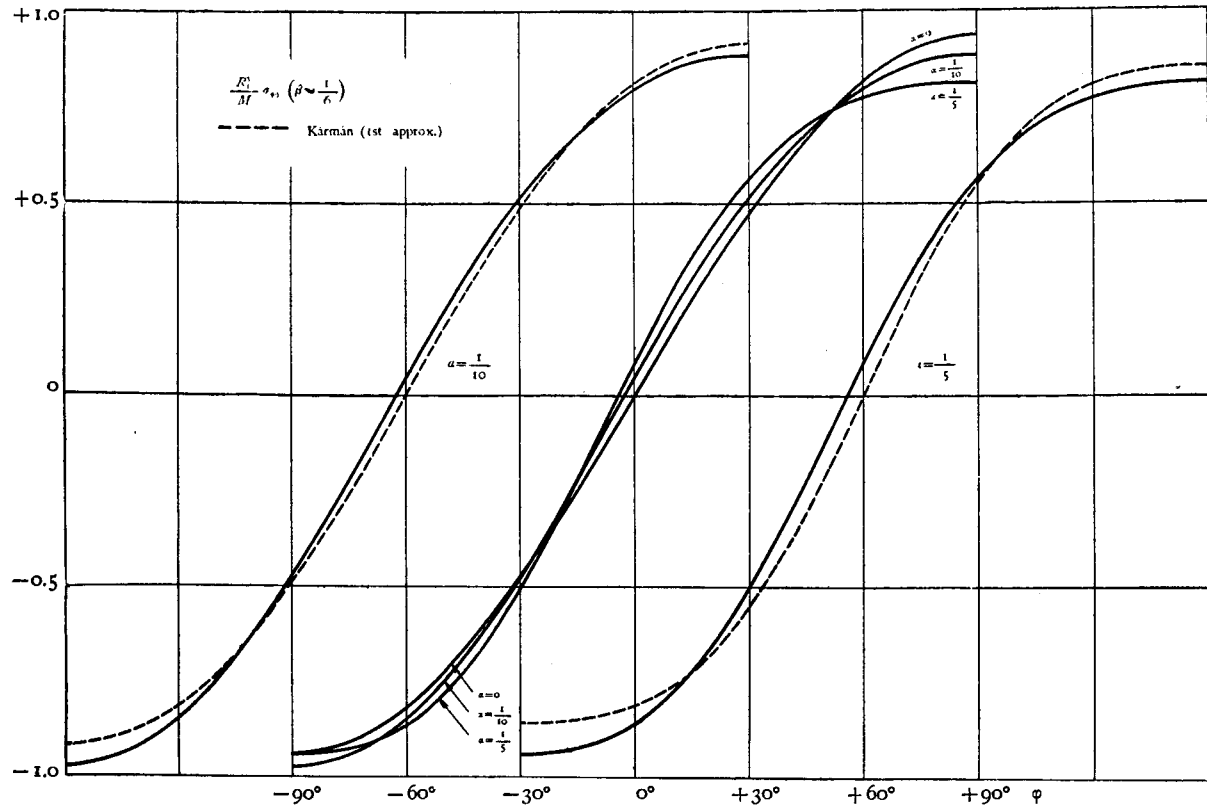


Fig. 9.

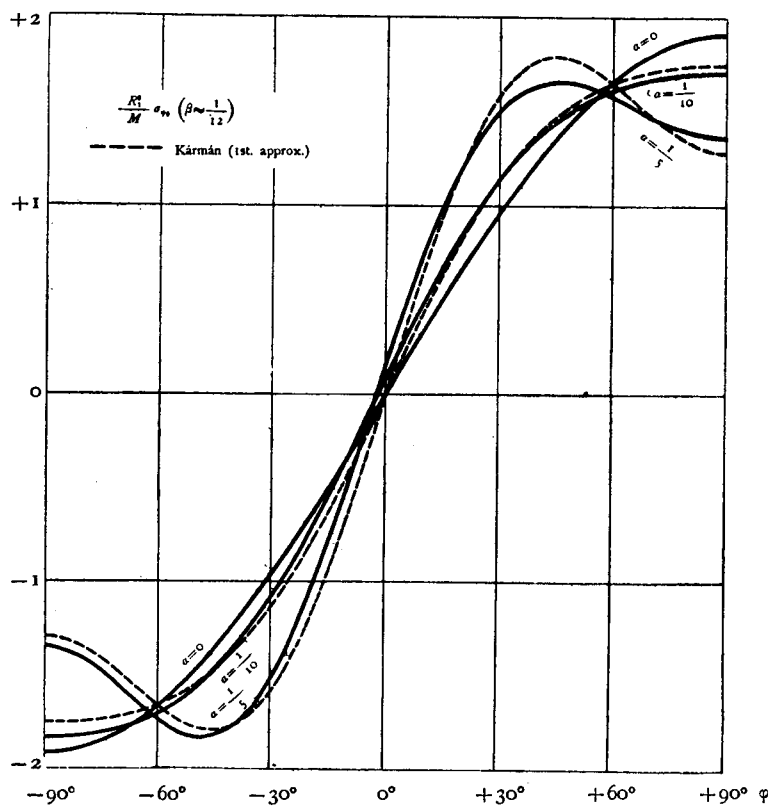


Fig. II.

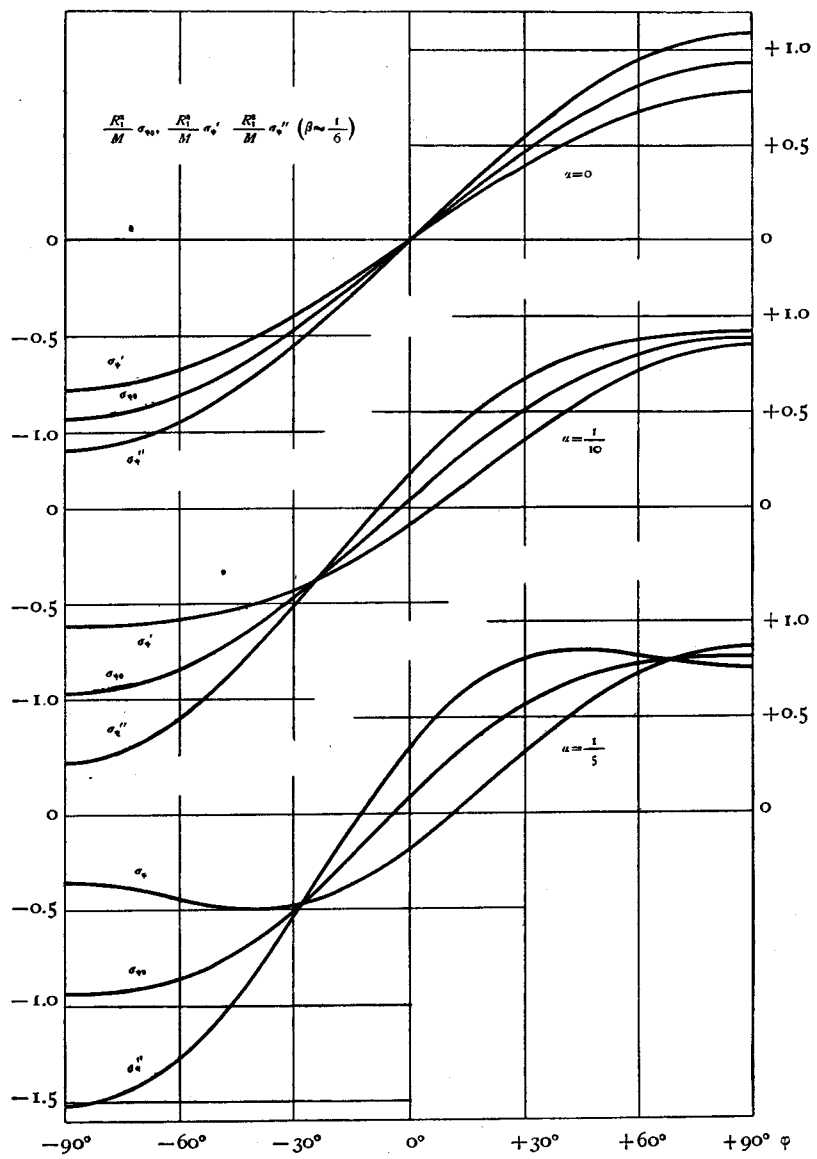


Fig. IO.

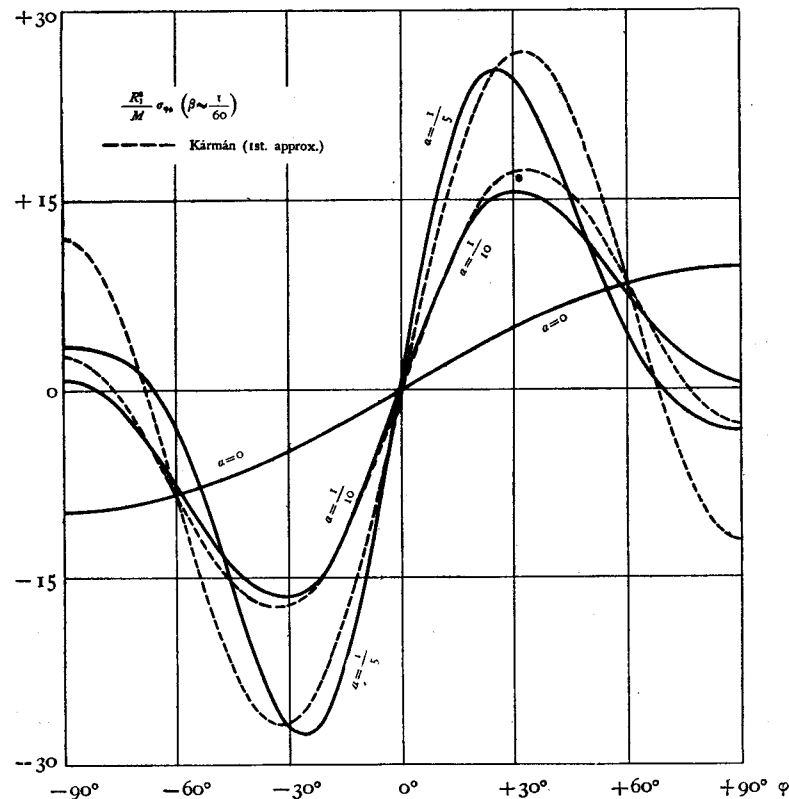


Fig. 12.

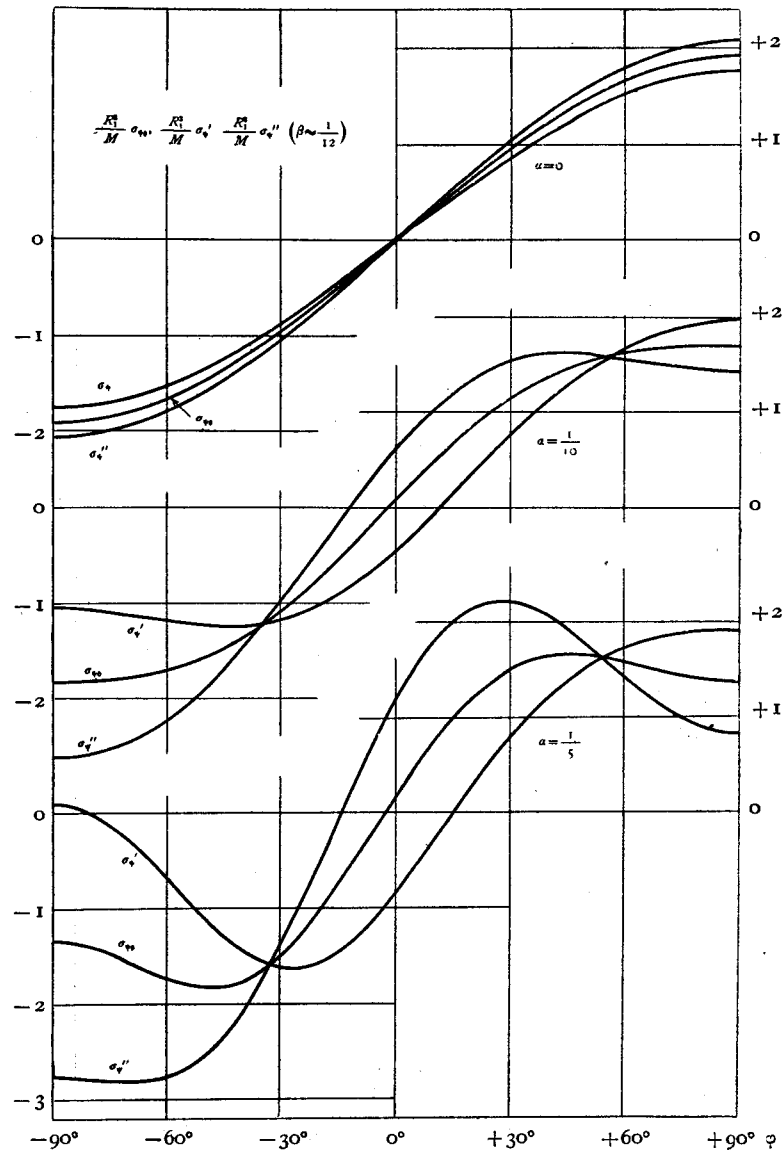


Fig. 13.

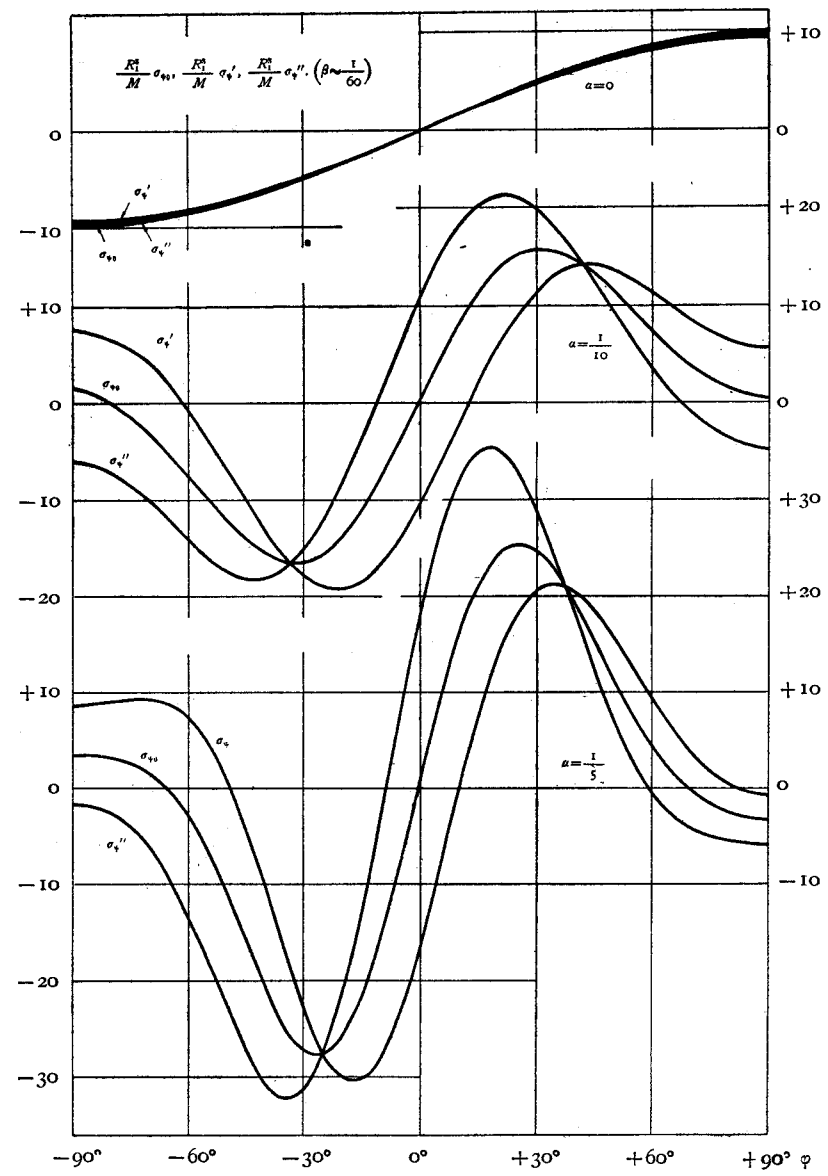


Fig. 14.

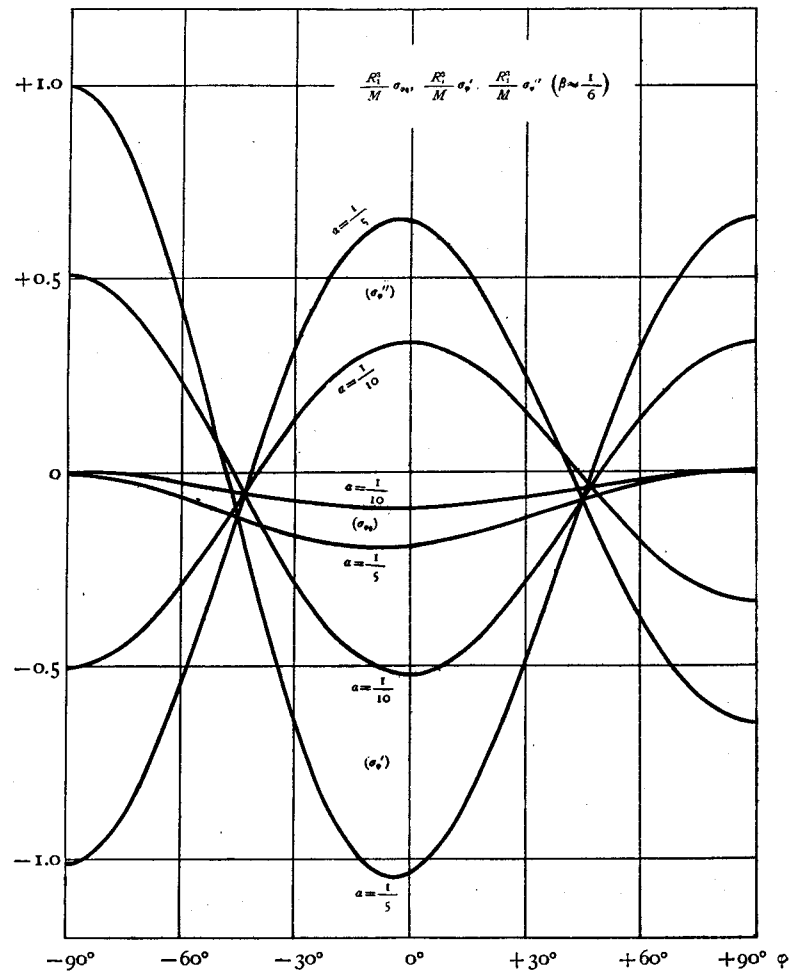


Fig. 15.

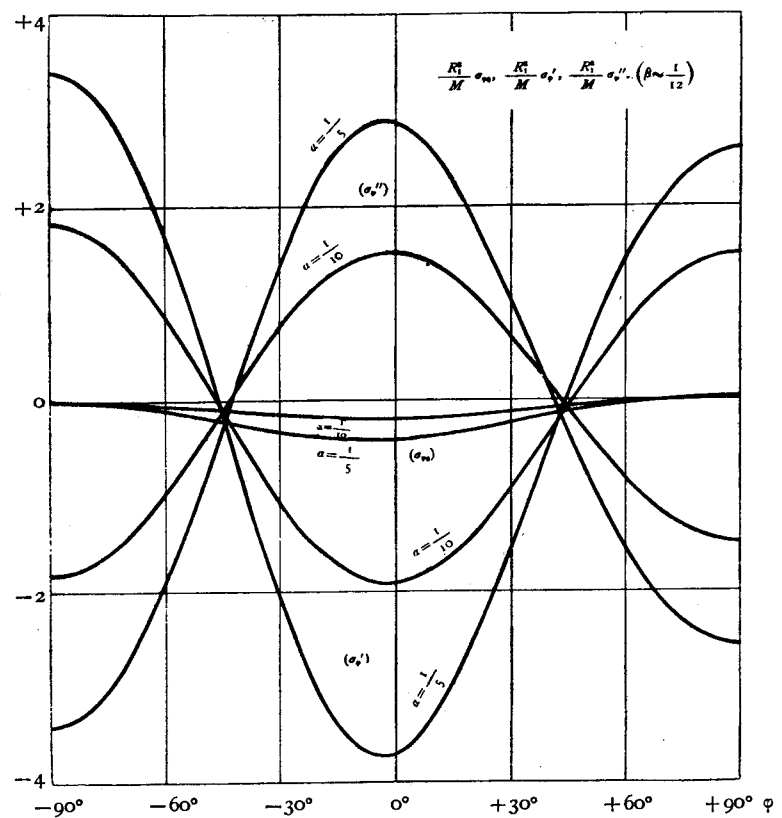


Fig. 16.

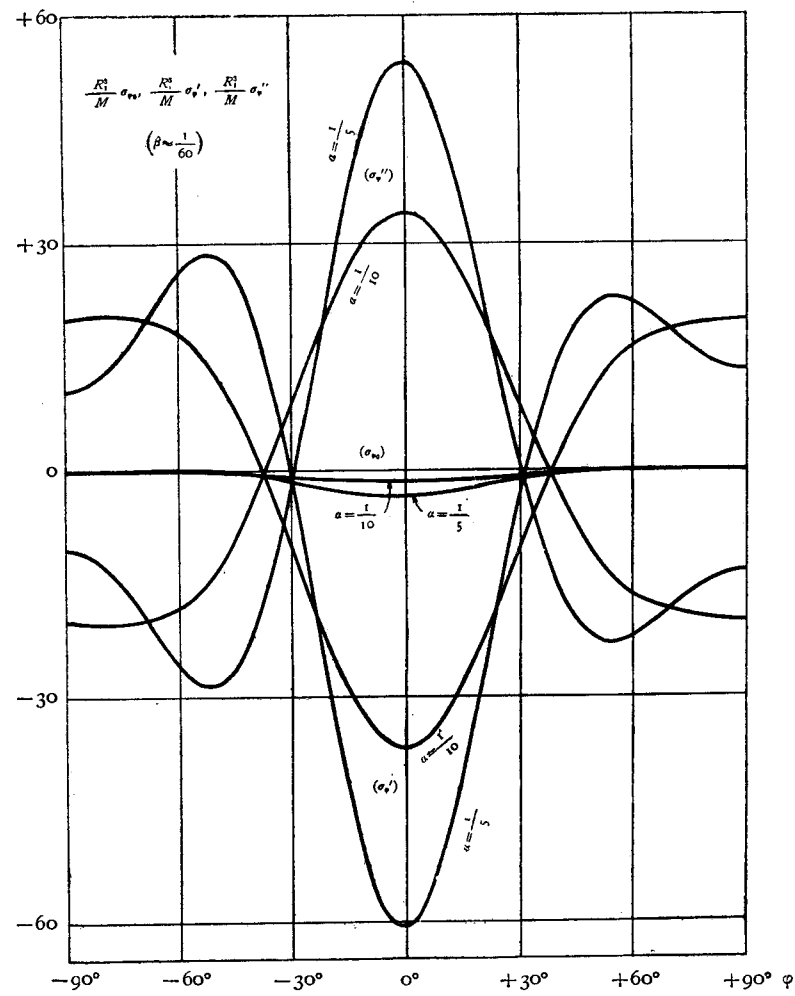


Fig. 17.

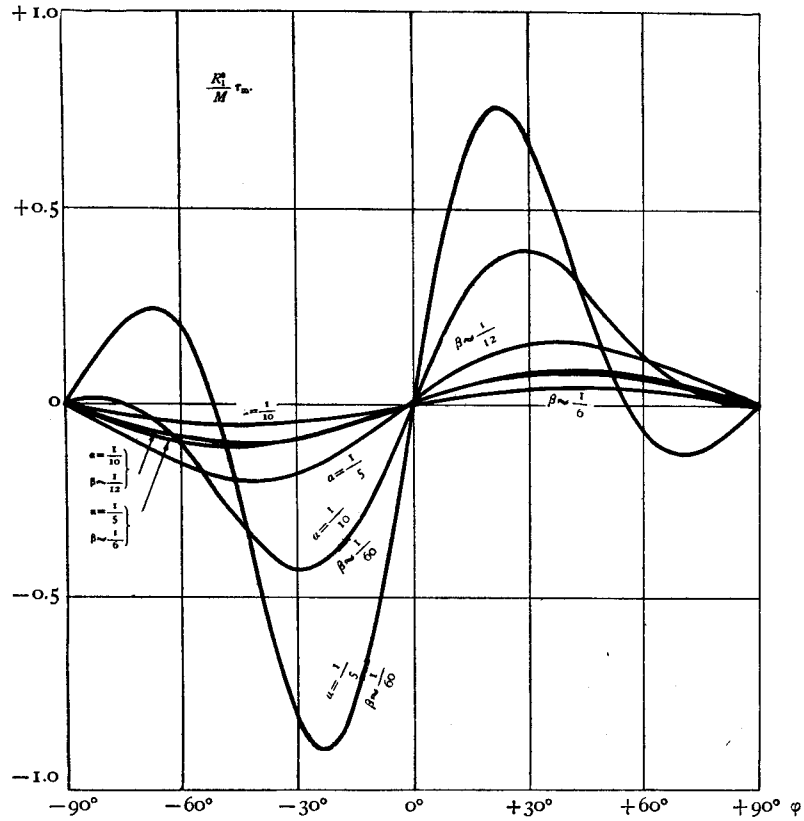


Fig. 18.

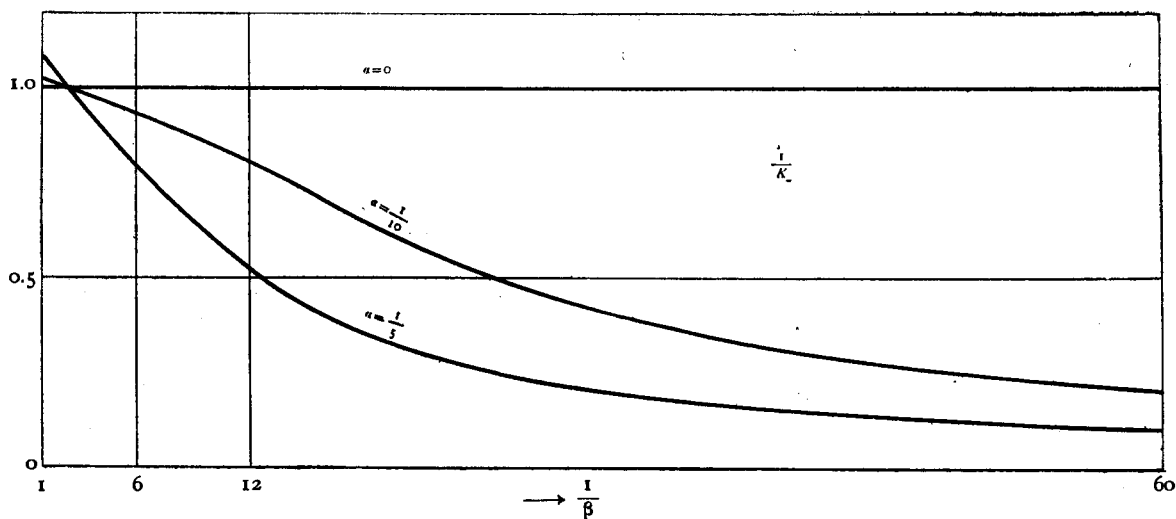


Fig. 19.

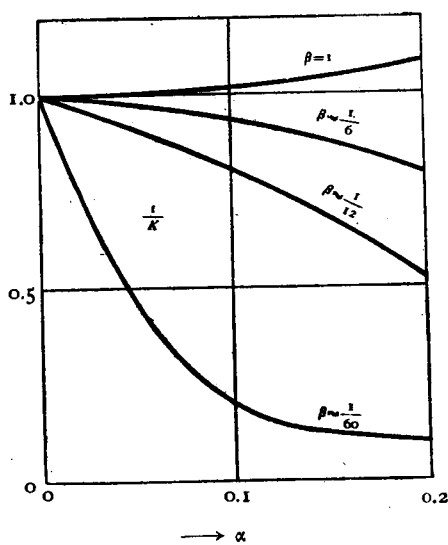


Fig. 20.

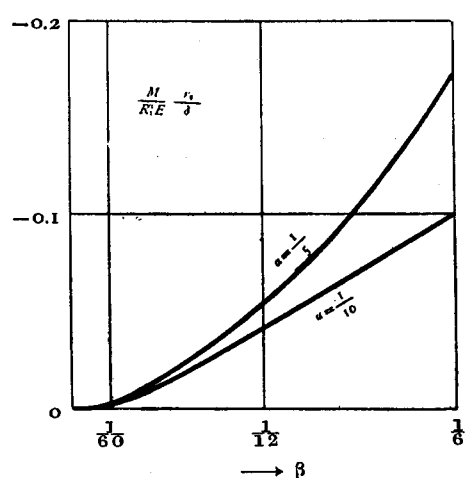


Fig. 21.

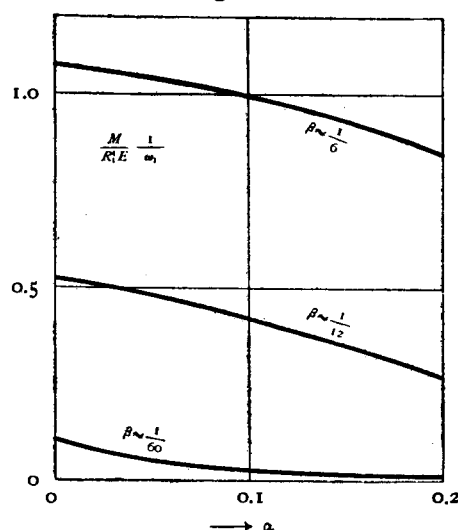


Fig. 22.

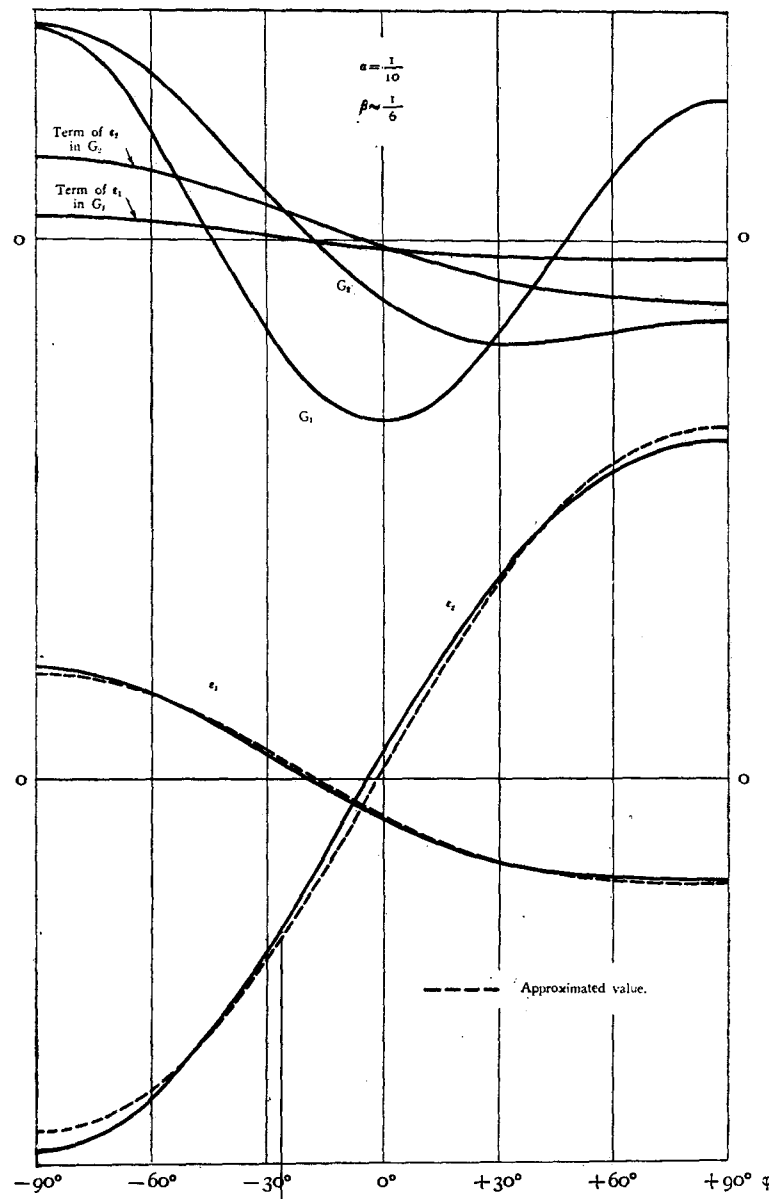


Fig. 23.

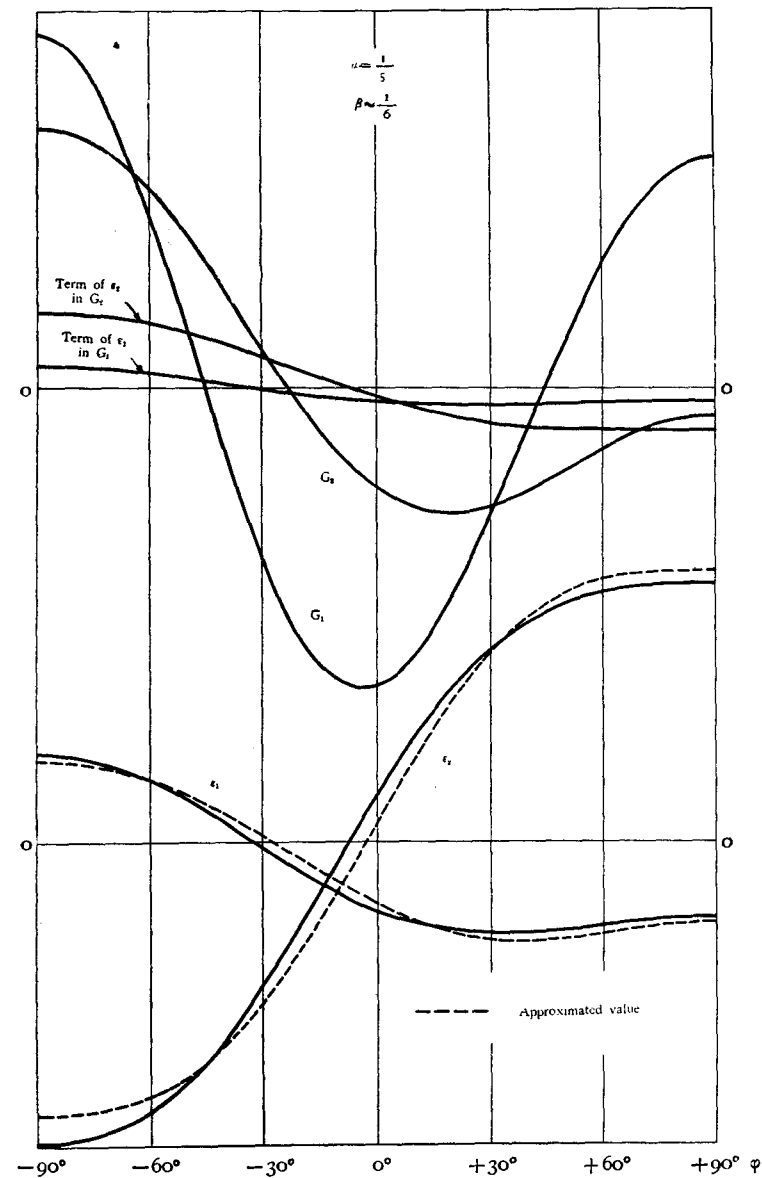


Fig. 24.

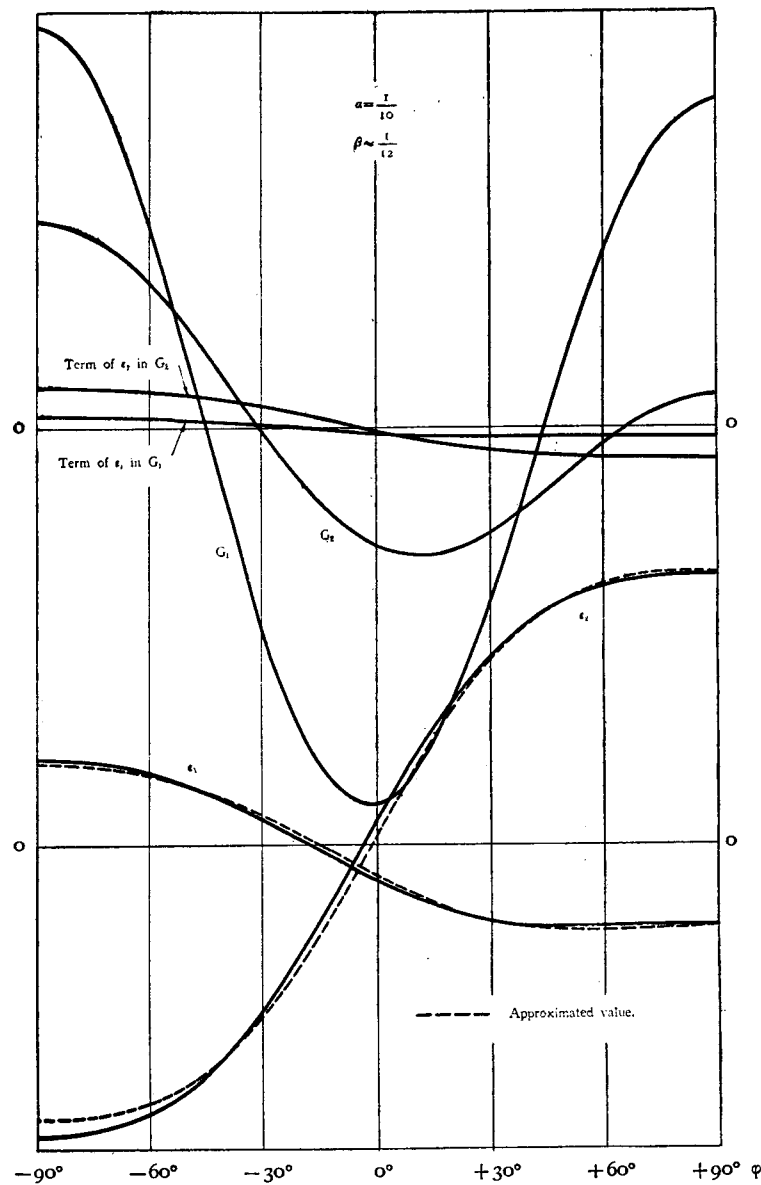


Fig. 25.

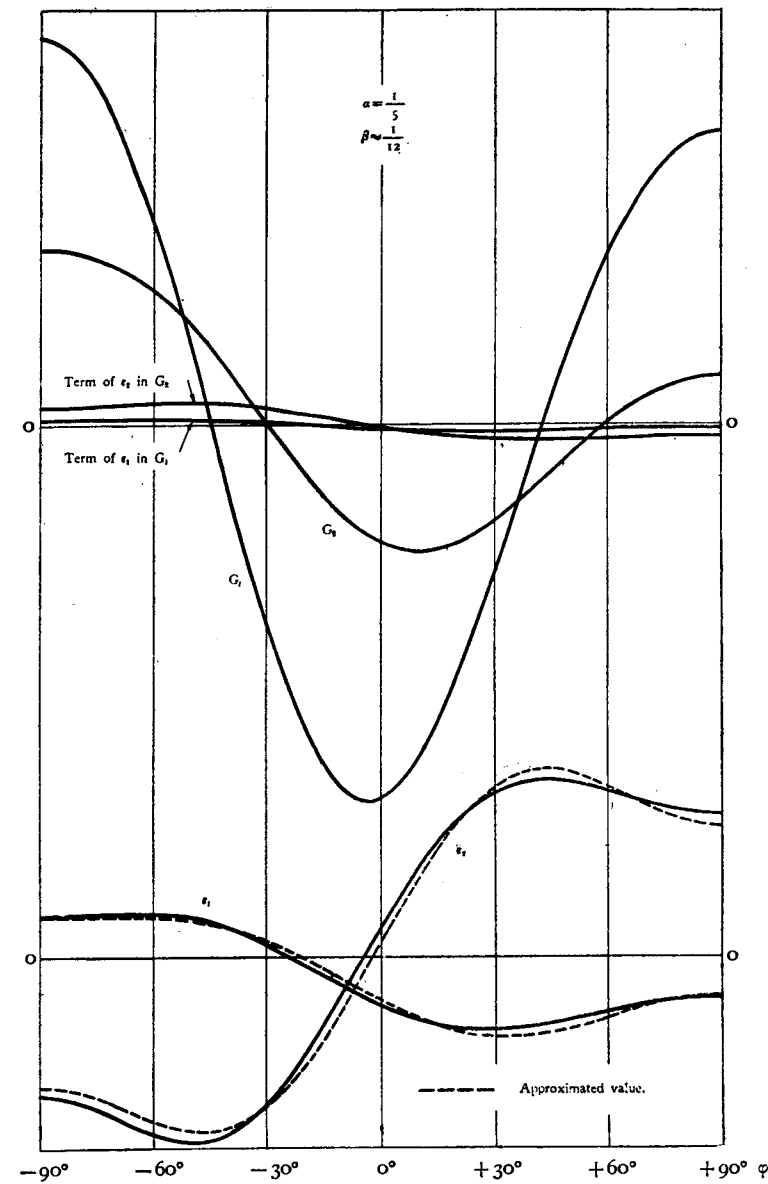
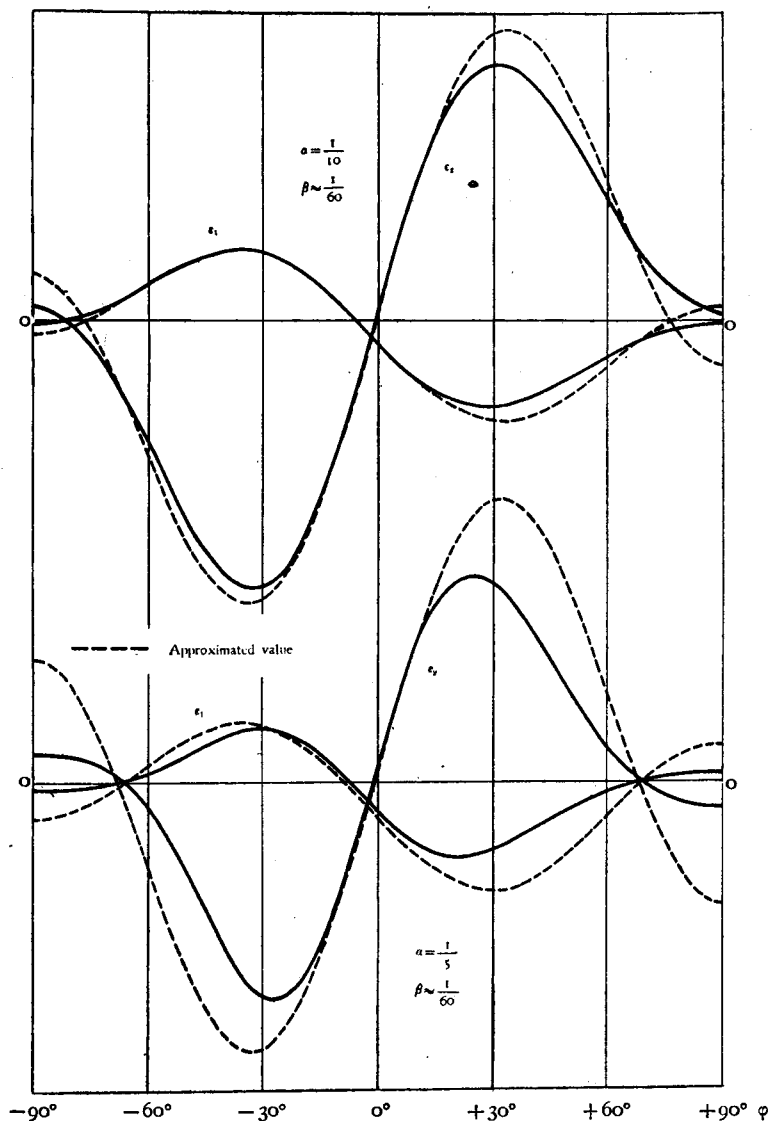


Fig. 26.



(Received Oct. 26, 1935).

# Mathematical Theories of Bourdon Pressure Tubes and Bending of Curved Pipes.

By Masasuke Tueda.

## Third Report: A Numerical Example of the Bourdon Tube.

The third report gives a numerical example of the Bourdon tube, along with an application of the theory to a cross-section which has straight parts in it as in the case of the flat type of the Bourdon tube.

### I. Application of the Theory to a Modified Form of $R_1^I = R_1^{IV} = \infty$ .

Recently, the flat type of Bourdon tubes as shown in Fig. 27 is used more widely than the elliptic type. In the flat type of the tube,  $R_1^I$  and  $R_1^{IV}$ , shown in Fig. 2 in the first report, are both equal to infinity, and the tube contains a pair of cylindrical surfaces in it. In order to show a numerical example of "Case I", and an application of the theory to a modified form of cross-section at the same time, we give numerical calculations on such a flat type of the Bourdon tube. For this purpose, we begin with the modifications of the formulae for the cylindrical parts, I and IV, in Fig. 27.

In each of these cylindrical parts of the pipe wall, the meridian section of the middle surface of the wall becomes a straight line, the length of which, measured from the plane of symmetry, is represented by the notation  $s$ . The greatest value of  $s$  is denoted by  $\ell$ . Then the required modifications of the formulae will be accomplished easily by the following substitutions of the values in formulae given in the first report.

$$\left. \begin{aligned} R_1 &= \infty, & R_1 d\varphi &= \mp ds, \\ \varphi &= \pm \frac{\pi}{2}, & \sin \varphi &= \pm 1, \quad \cos \varphi = 0, \end{aligned} \right\} \quad (180)$$

$$R_2 = \pm r, \quad w = \mp \eta, \quad u = \pm v,$$

where the upper sign of the double sign corresponds to part IV, and the lower sign to part I. In the following, we define the notation  $R_1$  to represent the radius in parts II and III, then

$$r^I = r_0 - R_1, \quad r^{IV} = r_0 + R_1. \quad (181)$$

Applying these substitutions to the equations (12), (13), (16), (21), (23) and (30) in the first report, we get

$$\left. \begin{aligned} \theta &= \mp \frac{dw}{ds} = \frac{d\eta}{ds}, \\ \epsilon_1 &= \mp \frac{du}{ds} = -\frac{dv}{ds}, \quad \text{or } v = - \int \epsilon_1 ds, \\ \epsilon_2 &= \omega_0 \mp \frac{w}{r} = \omega_0 + \frac{\eta}{r}, \quad \text{or } \eta = r(\epsilon_2 - \omega_0), \end{aligned} \right\} \quad (182)$$

$$\left. \begin{aligned} \epsilon_\varphi &= \epsilon_1 \pm z \frac{d\theta}{ds}, \\ \epsilon_\varphi &= \epsilon_2 \pm \frac{z}{r} (\epsilon_2 - \omega_0), \end{aligned} \right\} \quad (183)$$

$$r \frac{d\epsilon_2}{ds} = \theta, \quad (184)$$

$$\left. \begin{aligned} T_1 &= \text{const.} = \pm \left[ \frac{p}{2} \frac{(r \mp h)^2 - r_0^2}{r} + \frac{2h\tau_0 \omega_0}{r} \right], \\ T_2 &= r \frac{dN}{ds} \pm p(r \mp h), \end{aligned} \right\} \quad (185)$$

$$\frac{dG_1}{ds} \pm N = 0, \quad (186)$$

$$\left. \begin{aligned} G_1 &= \pm \frac{2h^3 E}{3(1-\mu^2)} \left( \frac{d\theta}{ds} - \frac{\mu \omega_0}{r} \right), \\ G_2 &= \pm \frac{2h^3 E}{3(1-\mu^2)} \left( \mu \frac{d\theta}{ds} - \frac{\omega_0}{r} \right). \end{aligned} \right\} \quad (187)$$

Using the variable  $V$  as before,

$$V = \pm Nr, \quad (188)$$

$$\left. \begin{aligned} \text{and } T_2 &= \pm \left[ \frac{dV}{ds} + p(r \mp h) \right], \\ N &= \pm \frac{V}{r}. \end{aligned} \right\} \quad (189)$$

Substitute the first equations of (185) and (189) into the equation (184) by the relation (111) in the first report, and also substitute equations (187) and (188) into the equation (186), then we have the differential equations for the present problem as follows:

$$\left. \begin{aligned} \frac{d^2 V}{ds^2} &= \pm \lambda_{1s} \theta, \\ \frac{d^2 \theta}{ds^2} &= \mp \lambda_{2s} V, \end{aligned} \right\} \quad (190)$$

$$\left. \begin{aligned} \text{where } \lambda_{1s} &= \frac{2hE}{r}, \\ \lambda_{2s} &= \frac{3(1-\mu^2)}{2h^3 r E}. \end{aligned} \right\} \quad (191)$$

Eliminating  $\theta$  and  $V$  respectively from the above equations, we get

$$\left. \begin{aligned} \frac{d^4 V}{ds^4} + 4n_s^4 V = 0, \\ \frac{d^4 \theta}{ds^4} + 4n_s^4 \theta = 0, \end{aligned} \right\} \quad (192)$$

where  $4n_s^4 = \lambda_{1s} \cdot \lambda_{2s} = \frac{3(1-\mu^2)}{r^2 h^2}$ , (193)

or  $n_s = \sqrt[4]{\frac{3(1-\mu^2)}{4r^2 h^2}}$ .

As before,  $\theta$  and  $V$  are composed of the same integrals, differing only by the values of the integration constants. We need, therefore, to solve only one of the two equations (192). The general solution of the equation of  $\theta$ , for example, may easily be written as follows :

$$\begin{aligned} \theta = & B_1 \cosh(n_s s) \sin(n_s s) + B_2 \sinh(n_s s) \cos(n_s s) \\ & + B_3 \cosh(n_s s) \cos(n_s s) \\ & + B_4 \sinh(n_s s) \sin(n_s s), \end{aligned} \quad (194)$$

where  $B_1, B_2, B_3$  and  $B_4$  are four integration constants. Then, from the second equation of (190), we have

$$\begin{aligned} V = & \mp \frac{1}{\lambda_{2s}} \frac{d^2 \theta}{ds^2} \\ = & \mp \frac{2n_s^2}{\lambda_{2s}} \left[ B_1 \sinh(n_s s) \cos(n_s s) \right. \\ & - B_2 \cosh(n_s s) \sin(n_s s) \\ & - B_3 \sinh(n_s s) \sin(n_s s) \\ & \left. + B_4 \cosh(n_s s) \cos(n_s s) \right]. \end{aligned} \quad (195)$$

Now, the boundary conditions at  $s=0$  are

$$\left. \begin{aligned} (\theta)_{s=0} = & \left( \frac{d\eta}{ds} \right)_{s=0} = (N)_{s=0} = 0, \\ (\theta)_{s=0} = & (V)_{s=0} = 0, \end{aligned} \right\} \quad (196)$$

from which we get  $B_3 = B_4 = 0$ .

Then, the required solution of the differential equations are given by

$$\left. \begin{aligned} \theta = & B_1 \cosh(n_s s) \sin(n_s s) \\ & + B_2 \sinh(n_s s) \cos(n_s s), \\ V = & \mp \frac{4rh^3 En_s^2}{3(1-\mu^2)} \left[ B_1 \sinh(n_s s) \cos(n_s s) \right. \\ & \left. - B_2 \cosh(n_s s) \sin(n_s s) \right]. \end{aligned} \right\} \quad (197)$$

All the values of  $T_1, T_2, N, G_1, G_2, \eta$  and  $\nu$  will be calculated easily by the above formulae.

In the case of the Bourdon tube, the terms with  $\epsilon_1$  and  $\epsilon_2$  in  $G_1$  and  $G_2$  are neglected altogether. By these neglects, the equations (139), (140), (141) and (142) in the second report become as shown in the following, which are applicable throughout the entire range of I, II, III and IV.

$$\left. \begin{aligned} \sigma'_\varphi = & \frac{T_1}{2h} + \frac{3G_1}{2h^2}, \\ \sigma_{\varphi 0} = & \frac{T_1}{2h}, \end{aligned} \right\} \quad (198)$$

$$\left. \begin{aligned} \sigma''_\varphi = & \frac{T_1}{2h} - \frac{3G_1}{2h^2}, \\ \sigma'_\psi = & \frac{T_2}{2h} + \frac{3G_2}{2h^2}, \\ \sigma_{\psi 0} = & \frac{T_2}{2h}, \\ \sigma''_\psi = & \frac{T_2}{2h} - \frac{3G_2}{2h^2}, \end{aligned} \right\} \quad (199)$$

$$\tau_m = \frac{N}{2h}. \quad (200)$$

Next we must consider the modifications of the boundary conditions.

(a). The conditions (a) at  $\varphi = \pm \frac{\pi}{2}$  in the first report correspond to those at  $s=0$  in the present case, which have been employed already in equations (196).

(b). The conditions (b) at  $\varphi = \pm \varphi_0$  correspond to those at  $\varphi = \pm \frac{\pi}{2}$  and  $s=l$  in the present case, and we must put  $+ \left( \frac{d\theta}{ds} \right)_B^I$  and  $- \left( \frac{d\theta}{ds} \right)_A^{IV}$  instead of  $\left( \frac{1}{R_1} \frac{d\theta}{d\varphi} \right)_B^I$  and  $\left( \frac{1}{R_1} \frac{d\theta}{d\varphi} \right)_A^{IV}$  respectively.

(c). The conditions (c) at  $\varphi = 0$  are applicable to the present case without any modification. It is more convenient, in the present case, to give the condition for  $\nu$  in the following form :

$$\begin{aligned} & - \int_0^l (\epsilon_1)^I ds + \int_{-\frac{\pi}{2}}^{+\frac{\pi}{2}} (\epsilon_1 \sin \varphi + \theta \cos \varphi) R_1 d\varphi \\ & - \int_l^0 (\epsilon_1)^{IV} ds = 0. \end{aligned} \quad (201)$$

(d). Lastly, the condition (d) for  $M$  is given, in the present case, by

$$\begin{aligned} & - \int_0^l (T_2 R_1 - G_2)^I ds \\ & + \int_{-\frac{\pi}{2}}^{+\frac{\pi}{2}} \{ T_2(r - r_0) - G_2 \sin \varphi \} R_1 d\varphi \\ & - \int_l^0 (T_2 R_1 - G_2)^{IV} ds = 0. \end{aligned} \quad (202)$$

## II. Process and Results of Numerical Calculations of a Flat Bourdon Tube.

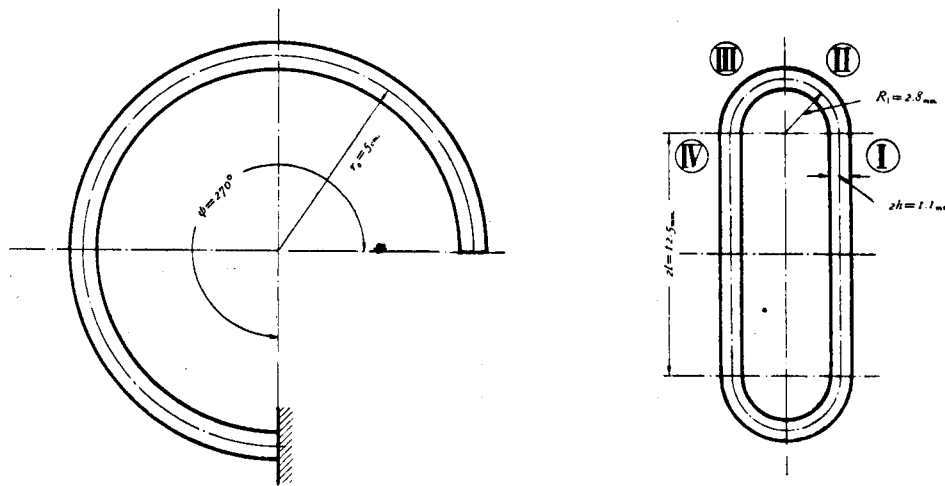
A tube from a real Bourdon gauge of 400 lbs. per sq. inch is taken up as a sample for the present numerical calculations. The dimensions of the tube are shown in Fig. 27 ; that is,

$$\begin{aligned} R_1 &= 2.8 \text{ mm}, & r_0 &= 50 \text{ mm}, & 2h &= 1.1 \text{ mm}, \\ 2l &= 12.5 \text{ mm}, & \varphi &= 270^\circ, \end{aligned}$$

and thence

$$\begin{aligned} \alpha &= 0.056, & n &= 8.40, \\ n_s^I &= 1.78 \left[ \frac{I}{cm.} \right], & n_s^{IV} &= 1.69 \left[ \frac{I}{cm.} \right]. \end{aligned}$$

Fig. 27.



The material of the tube is brass, the modulus of elasticity of which is assumed as  $E=800000 \text{ kg./cm}^2$ , and the Poisson's ratio  $\mu$  as  $\mu=0.3$ . The units of all the numerical values in the following calculations are derived from [cm.] and [kg].

First of all, we must determine all the infinite series in the solution for parts II and III, among which the first and the second integrals of the complementary functions of the general solutions are determined by the equations (48), (52), (56), (58), (74) and (76). The values of the coefficients

of these series are given in Table 19.

From the equations (81)<sub>I</sub>, (93), (94) and (101), the series in the particular integral are determined as containing  $\rho$  and the unknown constants  $\omega_0$  and  $\tau_0$  in them; that is, the coefficients of these series are given in the form of the sum of the three terms with  $\omega_0$ ,  $\tau_0$  and  $\rho$ .

$$\left. \begin{aligned} k_v^{**} &= k_{vw}^{**}\omega_0 + k_{vt}^{**}\tau_0 + k_{vp}^{**}\rho, \\ j_v^{**} &= j_{vw}^{**}\omega_0 + j_{vt}^{**}\tau_0 + j_{vp}^{**}\rho. \end{aligned} \right\} \quad (203)$$

Table 19.

v	First Integral.				Second Integral.			
	$k_v$	$j_v$	$nj_v + \mu k_v$	$\mu j_v - nk_v$	$k_v^*$	$j_v^*$	$nj_v^* + \mu k_v^*$	$\mu j_v^* - nk_v^*$
$+ \frac{\pi}{2} \geq \varphi \geq 0$								
0	+1.	0.	+0.3	-8.4	+1.	0.	+0.3	-8.4
1	0.	-0.4448	-3.736	-0.133	-0.3498	-0.1483	-1.351	+2.894
2	-0.0320	+0.0116	+0.088	+0.273	+0.1344	+0.0350	+0.335	-1.118
3	-0.0030	+0.0005	+0.003	+0.026	-0.0597	-0.0095	-0.098	+0.499
4	+0.0017	+0.0002	+0.002	-0.014	+0.0270	+0.0031	+0.034	-0.226
5	-0.0006	-0.0001	-0.001	+0.005	-0.0124	-0.0011	-0.013	+0.104
6	+0.0002			-0.002	+0.0057	+0.0004	+0.005	-0.048
7	-0.0001			+0.001	-0.0027	-0.0002	-0.002	+0.022
8					+0.0013	+0.0001	+0.001	-0.011
$0 \geq \varphi \geq -\frac{\pi}{2}$								
0	+1.	0.	+0.3	-8.4	+1.	0.	+0.3	-8.4
1	0.	-0.4983	-4.186	-0.150	+0.3139	-0.1663	-1.303	-2.687
2	-0.0402	+0.0146	+0.111	+0.342	+0.1189	-0.0266	-0.187	-1.007
3	+0.0076	+0.0005	+0.006	-0.064	+0.0545	-0.0085	-0.055	-0.461
4	+0.0013	-0.0005	-0.003	-0.011	+0.0244	-0.0030	-0.018	-0.206
5	+0.0005	-0.0001		-0.004	+0.0107	-0.0011	-0.006	-0.091
6	+0.0002			-0.002	+0.0050	-0.0004	-0.002	-0.042
7	+0.0001			-0.001	+0.0023	-0.0002	-0.001	-0.020
8					+0.0011	-0.0001		-0.009

Table 20.

$v$	$j_{vw}^{**}$	$j_{vt}^{**}$	$j_{vp}^{**}$	$\mu j_{vw}^{**} - nk_{vw}^{**}$	$\mu j_{vt}^{**} - nk_{vt}^{**}$	$\mu j_{vp}^{**} - nk_{vp}^{**}$
$+ \frac{\pi}{2} \geq \varphi \geq 0$						
0	0.	0.	0.	0.	0.	0.
1	+0.00530	+2.793 × 10 <sup>-5</sup>	0.	+1.235	+0.986 × 10 <sup>-5</sup>	+1.814 × 10 <sup>-6</sup>
2	+0.00424	-1.205 × "	+0.961 × 10 <sup>-8</sup>	-0.532	-1.427 × "	-0.809 × "
3	-0.00029	+0.518 × "	-0.194 × "	+0.228	+0.365 × "	+0.349 × "
4	-0.00039	-0.232 × "	+0.010 × "	-0.102	-0.081 × "	-0.157 × "
5	+0.00032	+0.106 × "	+0.018 × "	+0.047	+0.014 × "	+0.072 × "
6	-0.00019	-0.049 × "	-0.015 × "	-0.022	+0.001 × "	-0.033 × "
7	+0.00010	+0.023 × "	+0.009 × "	+0.010	-0.003 × "	+0.015 × "
8	-0.00005	-0.011 × "	-0.005 × "	-0.005	+0.002 × "	-0.007 × "
$0 \geq \varphi \geq -\frac{\pi}{2}$						
0	0.	0.	0.	0.	0.	0.
1	-0.00594	-3.128 × 10 <sup>-5</sup>	0.	-1.377	-0.753 × 10 <sup>-5</sup>	-2.271 × 10 <sup>-6</sup>
2	-0.01033	-1.141 × "	-1.349 × 10 <sup>-8</sup>	-0.503	+0.977 × "	-0.793 × "
3	-0.00163	-0.492 × "	-0.103 × "	-0.217	-0.028 × "	-0.343 × "
4	-0.00039	-0.221 × "	+0.005 × "	-0.097	-0.067 × "	-0.154 × "
5	-0.00006	-0.097 × "	+0.020 × "	-0.043	-0.047 × "	-0.067 × "
6	+0.00001	-0.045 × "	+0.015 × "	-0.020	-0.028 × "	-0.031 × "
7	+0.00002	-0.021 × "	+0.009 × "	-0.009	-0.015 × "	-0.015 × "
8	+0.00001	-0.010 × "	+0.005 × "	-0.005	-0.008 × "	-0.007 × "

Table 20 gives the numerical values of these coefficients in the present case. In the following, we make distinctions between the coefficients of  $\omega_0$ ,  $\tau_0$  and  $\rho$  by adding the suffix  $w$ ,  $t$  and  $p$  respectively. Then the series in the particular integrals are determined in the following form :

$$\left. \begin{aligned} \theta_2 &= \theta_{2w}\omega_0 + \theta_{2t}\tau_0 + \theta_{2p}\rho, \\ V_{2w} &= V_{2w}\omega_0 + V_{2t}\tau_0 + V_{2p}\rho, \end{aligned} \right\} \quad (204)$$

where  $\theta_{2w}$ ,  $\theta_{2t}$ ,  $V_{2w}$  and  $V_{2t}$  are given by the equations (153) in the second report, and  $\theta_{2p}$  and  $V_{2p}$  by the following similar equations :

$$\left. \begin{aligned} \theta_{2p} &= \cos \varphi \sum_{v=0}^{\infty} j_{vp}^{**} (\sin \varphi \mp 1)^v, \\ V_{2p} &= \cos \varphi \sum_{v=0}^{\infty} (\mu j_{vp}^{**} - nk_{vp}^{**}) (\sin \varphi \mp 1)^v. \end{aligned} \right\} \quad (205)$$

Since all the series in parts II and III are thus obtained, we must next determine the integration constants from the boundary conditions at  $\varphi=0$  and  $\varphi=\pm\frac{\pi}{2}$  or  $s=l$ . The values of the series at  $\varphi=0$  are given by the equations (154) and (155) in the second report; those corresponding to the terms of  $\rho$  can be obtained by replacing the suffix  $w$  or  $t$  by  $\rho$ . Further, the values of the series at  $\varphi=\pm\frac{\pi}{2}$  become as follows :

$$\left. \begin{aligned} (\theta_{1,1})_{\pm\frac{\pi}{2}} &= k_0 = +1, \\ \left( \frac{d\theta_{1,3}}{d\varphi} \right)_{\pm\frac{\pi}{2}} &= \mp k_0^* = \mp 1, \\ (V_{1,1})_{\pm\frac{\pi}{2}} &= (nj_0 + \mu k_0) = +\mu, \\ \left( \frac{dV_{1,3}}{d\varphi} \right)_{\pm\frac{\pi}{2}} &= \mp (nj_0^* + \mu k_0^*) = \mp \mu, \\ (V_{1,2})_{\pm\frac{\pi}{2}} &= (\mu j_0 - nk_0) = -n, \\ \left( \frac{dV_{1,4}}{d\varphi} \right)_{\pm\frac{\pi}{2}} &= \mp (\mu j_0^* - nk_0^*) = \pm n. \end{aligned} \right\} \quad (206)$$

All the other series become zero at  $\varphi=\pm\frac{\pi}{2}$ .

Table 21 shows their values in the present case. Numerical values at  $s=l$  for parts I and IV, which give the boundary conditions employed here, will be obtained easily by the formulae in the previous chapter. Then the equations (120) and the first four of the equations (121) offer twelve equations containing twelve unknown integration constants  $B_1^I$ ,  $B_2^I$ ,  $B_1^{II}$ ,  $B_2^{II}$ ,  $B_3^{II}$ ,  $B_4^{II}$ ,  $B_1^{III}$ ,  $B_2^{III}$ ,  $B_3^{III}$ ,  $B_4^{III}$ ,  $B_1^{IV}$  and  $B_2^{IV}$  for the whole range of I, II, III and IV; and, solving these twelve simultaneous equations, we can determine the values of all the integration constants in the form of the sum of the three terms with  $\omega_0$ ,  $\tau_0$  and  $\rho$ ; that is,

$$B_i^X = B_{iw}^X \omega_0 + B_{it}^X \tau_0 + B_{ip}^X \rho, \quad (i=1, 2, 3, 4), \quad (X=I, IV), \quad (i=1, 2, 3, 4). \quad (207)$$

In Table 22, their values for the present case are shown.

Table 21.

	at $\varphi = +\frac{\pi}{2}$	at $\varphi = +0$	at $\varphi = -0$	at $\varphi = -\frac{\pi}{2}$		at $\varphi = +\frac{\pi}{2}$	at $\varphi = +0$	at $\varphi = -0$	at $\varphi = -\frac{\pi}{2}$
$\theta_{1,1}$	+ 1	+ 0.9736	+ 0.9695	+ 1	$\frac{d\theta_{1,1}}{d\varphi}$	0.	+ 0.0427	- 0.0473	0.
$\theta_{1,2}$	0.	+ 0.4562	- 0.4838	0.	$\frac{d\theta_{1,2}}{d\varphi}$	0.	- 0.4680	- 0.4699	0.
$\theta_{1,3}$	0.	+ 1.5943	+ 1.5319	0.	$\frac{d\theta_{1,3}}{d\varphi}$	- 1.	- 1.0411	+ 0.9307	+ 1.
$\theta_{1,4}$	0.	+ 0.1978	- 0.2063	0.	$\frac{d\theta_{1,4}}{d\varphi}$	0.	- 0.2692	- 0.2678	0.
$\theta_{2w}$	0.	- 0.00189	- 0.01831	0.	$\frac{d\theta_{2w}}{d\varphi}$	0.	+ 0.00186	- 0.03303	0.
$\theta_{2t}$	0.	- 4.948 $\times 10^{-5}$	- 5.165 $\times 10^{-5}$	0.	$\frac{d\theta_{2t}}{d\varphi}$	0.	+ 8.840 $\times 10^{-5}$	- 8.833 $\times 10^{-5}$	0.
$\theta_{2p}$	0.	+ 1.113 $\times 10^{-8}$	- 1.393 $\times 10^{-8}$	0.	$\frac{d\theta_{2p}}{d\varphi}$	0.	- 2.218 $\times 10^{-8}$	- 2.660 $\times 10^{-8}$	0.
$V_{1,1}$	+ 0.3	+ 4.124	- 3.772	+ 0.3	$\frac{dV_{1,1}}{d\varphi}$	0.	- 3.918	- 3.962	0.
$V_{1,2}$	- 8.4	- 8.042	- 8.290	- 8.4	$\frac{dV_{1,2}}{d\varphi}$	0.	- 0.499	+ 0.256	0.
$V_{1,3}$	0.	+ 2.140	- 1.272	0.	$\frac{dV_{1,3}}{d\varphi}$	- 0.3	- 2.574	- 1.970	+ 0.3
$V_{1,4}$	0.	- 13.333	- 12.932	0.	$\frac{dV_{1,4}}{d\varphi}$	+ 8.4	+ 8.663	- 7.899	- 8.4
$V_{2w}$	0.	- 2.186	- 2.276	0.	$\frac{dV_{2w}}{d\varphi}$	0.	+ 3.905	- 3.899	0.
$V_{2t}$	0.	- 2.865 $\times 10^{-5}$	+ 0.023 $\times 10^{-5}$	0.	$\frac{dV_{2t}}{d\varphi}$	0.	+ 5.272 $\times 10^{-5}$	+ 0.221 $\times 10^{-5}$	0.
$V_{2p}$	0.	- 3.263 $\times 10^{-6}$	- 3.688 $\times 10^{-6}$	0.	$\frac{dV_{2p}}{d\varphi}$	0.	+ 5.890 $\times 10^{-6}$	- 6.240 $\times 10^{-6}$	0.

Table 22.

	$B_1$	$B_2$	$B_3$	$B_4$
I	$B_{1w}^I = -0.06689$ $B_{1t}^I = +6.583 \times 10^{-5}$ $B_{1p}^I = +4.979 \times 10^{-5}$	$B_{2w}^I = -0.3482$ $B_{2t}^I = -1.605 \times 10^{-5}$ $B_{2p}^I = +3.607 \times 10^{-4}$		
II	$B_{1w}^{II} = -0.3100$ $B_{1t}^{II} = +9.018 \times 10^{-5}$ $B_{1p}^{II} = +2.915 \times 10^{-4}$	$B_{2w}^{II} = -0.4997$ $B_{2t}^{II} = -6.065 \times 10^{-5}$ $B_{2p}^{II} = +5.283 \times 10^{-4}$	$B_{3w}^{II} = +0.01767$ $B_{3t}^{II} = +6.846 \times 10^{-5}$ $B_{3p}^{II} = -3.744 \times 10^{-5}$	$B_{4w}^{II} = -0.3506$ $B_{4t}^{II} = +2.446 \times 10^{-6}$ $B_{4p}^{II} = -1.006 \times 10^{-4}$
III	$B_{1w}^{III} = +0.3116$ $B_{1t}^{III} = +9.375 \times 10^{-5}$ $B_{1p}^{III} = -2.921 \times 10^{-4}$	$B_{2w}^{III} = -0.4800$ $B_{2t}^{III} = +5.933 \times 10^{-5}$ $B_{2p}^{III} = +5.546 \times 10^{-4}$	$B_{3w}^{III} = +0.005143$ $B_{3t}^{III} = +6.341 \times 10^{-5}$ $B_{3p}^{III} = +2.697 \times 10^{-5}$	$B_{4w}^{III} = -0.3432$ $B_{4t}^{III} = -2.059 \times 10^{-6}$ $B_{4p}^{III} = -1.107 \times 10^{-4}$
IV	$B_{1w}^{IV} = +0.06303$ $B_{1t}^{IV} = +6.990 \times 10^{-5}$ $B_{1p}^{IV} = -3.291 \times 10^{-5}$	$B_{2w}^{IV} = +0.3587$ $B_{2t}^{IV} = -6.601 \times 10^{-6}$ $B_{2p}^{IV} = -3.951 \times 10^{-4}$		

$\theta$ ,  $V_s$  and their derivatives in the equations (104) and (105) in the first report are then determined in the form of the sum of three infinite series as follows:

$$\left. \begin{aligned} \theta &= \theta_w \omega_0 + \theta_t \tau_0 + \theta_p p, \\ V_s &= V_{sw} \omega_0 + V_{st} \tau_0 + V_{sp} p, \\ \frac{d\theta}{d\varphi} &= \frac{d\theta_w}{d\varphi} \omega_0 + \frac{d\theta_t}{d\varphi} \tau_0 + \frac{d\theta_p}{d\varphi} p, \\ \frac{dV_s}{d\varphi} &= \frac{dV_{sw}}{d\varphi} \omega_0 + \frac{dV_{st}}{d\varphi} \tau_0 + \frac{dV_{sp}}{d\varphi} p, \end{aligned} \right\} \quad (208)$$

$$\left. \begin{aligned} \text{where } \theta_w &= \sum_{v=0}^{\infty} a_{vw} (\sin \varphi \mp 1)^v \\ &\quad + \cos \varphi \sum_{v=0}^{\infty} a_{vw}^* (\sin \varphi \mp 1)^v, \\ V_{sw} &= \sum_{v=0}^{\infty} b_{vw} (\sin \varphi \mp 1)^v \\ &\quad + \cos \varphi \sum_{v=0}^{\infty} b_{vw}^* (\sin \varphi \mp 1)^v, \end{aligned} \right\} \quad (209)$$

Table 23.

$v$	$a_{vw}$	$a_{vw}^*$	$a_{vt}$	$a_{vt}^*$	$a_{vp}$	$a_{vp}^*$
$+ \frac{\pi}{2} \geq \varphi \geq 0$						
0	+0.3116	+0.0051	+9.375 $\times 10^{-5}$	+6.341 $\times 10^{-5}$	-2.921 $\times 10^{-4}$	+0.270 $\times 10^{-4}$
1	+0.2135	+0.0544	-2.639 X "	+0.606 X "	-2.467 X "	+0.070 X "
2	-0.0156	-0.0071	-0.231 X "	-0.360 X "	+0.157 X "	-0.002 X "
3	-0.0011	+0.0027	-0.025 X "	+0.141 X "	+0.012 X "	-0.006 X "
4	+0.0004	-0.0013	+0.017 X "	-0.062 X "	-0.004 X "	+0.004 X "
5	-0.0002	+0.0006	-0.007 X "	+0.027 X "	+0.001 X "	-0.002 X "
6	+0.0001	-0.0003	+0.002 X "	-0.013 X "	-0.001 X "	+0.001 X "
7		+0.0002	-0.001 X "	+0.006 X "		-0.001 X "
8		-0.0001		-0.003 X "		
$0 \geq \varphi \geq -\frac{\pi}{2}$						
0	-0.3100	+0.0177	+9.018 $\times 10^{-5}$	+6.846 $\times 10^{-5}$	+2.915 $\times 10^{-4}$	-0.374 $\times 10^{-4}$
1	+0.2490	+0.0579	+3.022 X "	-1.020 X "	-2.633 X "	+0.050 X "
2	+0.0052	+0.0011	-0.452 X "	-0.334 X "	-0.040 X "	-0.018 X "
3	-0.0027	+0.0023	+0.066 X "	-0.121 X "	+0.025 X "	-0.012 X "
4	-0.0001	+0.0011	+0.015 X "	-0.055 X "	+0.001 X "	-0.006 X "
5	-0.0001	+0.0005	+0.006 X "	-0.024 X "		-0.003 X "
6		+0.0002	+0.002 X "	-0.011 X "		-0.002 X "
7		+0.0001	+0.001 X "	-0.005 X "		-0.001 X "
8		+0.0001		-0.002 X "		

Table 24.

$v$	$b_{vw}$	$b_{vw}^*$	$b_{vt}$	$b_{vt}^*$	$b_{vp}$	$b_{vp}^*$
$+ \frac{\pi}{2} \geq \varphi \geq 0$						
0	+4.135	+2.885	-4.703 $\times 10^{-4}$	+0.363 $\times 10^{-4}$	-4.747 $\times 10^{-3}$	+0.938 $\times 10^{-3}$
1	-1.100	+0.235	-3.582 X "	-0.818 X "	+1.017 X "	-0.355 X "
2	-0.104	-0.146	+0.245 X "	+0.093 X "	+0.125 X "	+0.132 X "
3	-0.011	+0.055	+0.018 X "	-0.036 X "	+0.013 X "	-0.058 X "
4	+0.008	-0.024	-0.006 X "	+0.018 X "	-0.009 X "	+0.026 X "
5	-0.002	+0.011	+0.002 X "	-0.009 X "	+0.003 X "	-0.012 X "
6	+0.001	-0.005	-0.001 X "	+0.004 X "	-0.001 X "	+0.005 X "
7		+0.002	+0.001 X "	-0.002 X "	+0.001 X "	-0.003 X "
8		-0.001		+0.001 X "		+0.001 X "
$0 \geq \varphi \geq -\frac{\pi}{2}$						
0	+4.104	+2.950	+5.366 $\times 10^{-4}$	-0.000 X $\times 10^{-4}$	-4.351 $\times 10^{-3}$	+0.834 $\times 10^{-3}$
1	+1.373	-0.458	-3.684 X "	-1.033 X "	-1.299 X "	+0.317 X "
2	-0.205	-0.153	-0.107 X "	-0.055 X "	+0.213 X "	+0.108 X "
3	+0.030	-0.056	+0.034 X "	-0.052 X "	-0.032 X "	+0.048 X "
4	+0.007	-0.025	+0.004 X "	-0.024 X "	-0.007 X "	+0.021 X "
5	+0.002	-0.011	+0.002 X "	-0.011 X "	-0.002 X "	+0.009 X "
6	+0.001	-0.005	+0.001 X "	-0.005 X "	-0.001 X "	+0.004 X "
7	+0.001	-0.002	+0.001 X "	-0.003 X "	-0.001 X "	+0.002 X "
8		-0.001		-0.001 X "		+0.001 X "

$$\left. \begin{aligned} \frac{d\theta_w}{d\varphi} &= \cos \varphi \sum_{v=1}^{\infty} v a_{vw} (\sin \varphi \mp 1)^{v-1} \\ &+ \cos^2 \varphi \sum_{v=1}^{\infty} v a_{vw}^* (\sin \varphi \mp 1)^{v-1} \\ &- \sin \varphi \sum_{v=0}^{\infty} a_{vw}^* (\sin \varphi \mp 1)^v, \\ \frac{dV_{tw}}{d\varphi} &= \cos \varphi \sum_{v=1}^{\infty} v b_{vw} (\sin \varphi \mp 1)^{v-1} \\ &+ \cos^2 \varphi \sum_{v=1}^{\infty} v b_{vw}^* (\sin \varphi \mp 1)^{v-1} \\ &- \sin \varphi \sum_{v=0}^{\infty} b_{vw}^* (\sin \varphi \mp 1)^v, \end{aligned} \right\} \quad (210)$$

and

$$\left. \begin{aligned} a_{vw} &= B_{1w} k_v + B_{2w} j_v, \\ a_{vw}^* &= B_{3w} k_v^* + B_{4w} j_v^* + j_{vw}^{**}, \\ b_{vw} &= B_{1w} (n j_v + \mu k_v) + B_{2w} (\mu j_v - n k_v), \\ b_{vw}^* &= B_{3w} (n j_v^* + \mu k_v^*) + B_{4w} (\mu j_v^* - n k_v^*) \\ &\quad + (\mu j_{vw}^{**} - n k_{vw}^{**}). \end{aligned} \right\} \quad (211)$$

The expressions for the terms with  $\tau_0$  and  $p$  are given by replacing the suffix  $w$  by  $t$  and  $p$  respec-

tively in the equations (209), (210) and (211). In Table 23 and Table 24, all the coefficients given by the equations (211) are shown.

In the last process of the calculations, we must determine the values of  $\omega_0$  and  $\tau_0$  by the boundary conditions (201) and (202), in which the integration in parts II and III must be done by numerical integration. For that purpose, we now calculate the values of each series at each angle of  $\varphi$ , with the angles at suitable equal intervals, as shown in Table 25. Calculating the values of  $\epsilon_1$ ,  $\theta$ ,  $T_2$  and  $G_2$  in the form of the sum of the three terms with  $\omega_0$ ,  $\tau_0$  and  $p$ , and inserting them in the equations (201) and (202), we can get two simultaneous equations of  $\omega_0$ ,  $\tau_0$  and  $p$ , which determine the required values of  $\omega_0$  and  $\tau_0$  as follows:

$$\left. \begin{aligned} \omega_0 &= -0.0007172 p, \\ \tau_0 &= +0.1273 p. \end{aligned} \right.$$

The problem is thus solved perfectly, and  $\theta$ ,  $V_s$  and their derivatives for parts II and III are determined as shown in Table 26, and  $\theta$ ,  $V$  and their derivatives for parts I and IV are given by the equations (212) and (213).

Table 25.

$\varphi$	$\theta_w$	$\theta_t$	$\theta_p$	$V_{tw}$	$V_{st}$	$V_{sp}$
-90°	-0.3100	+0.902 × 10 <sup>-4</sup>	+2.915 × 10 <sup>-4</sup>	+4.104	+5.366 × 10 <sup>-4</sup>	-4.351 × 10 <sup>-3</sup>
-60°	-0.2639	+1.277 × "	+2.378 × "	+5.727	+4.801 × "	-4.082 × "
-30°	-0.1436	+1.582 × "	+1.284 × "	+7.060	+3.035 × "	-4.063 × "
0°	+0.0225	+1.695 × "	-0.101 × "	+7.555	+0.437 × "	-4.136 × "
+30°	+0.1801	+1.577 × "	-1.446 × "	+7.018	-2.160 × "	-4.224 × "
+60°	+0.2816	+1.285 × "	-2.458 × "	+5.706	-3.982 × "	-4.387 × "
+90°	+0.3116	+0.938 × "	-2.921 × "	+4.135	-4.703 × "	-4.747 × "

$\varphi$	$\frac{d\theta_w}{d\varphi}$	$\frac{d\theta_t}{d\varphi}$	$\frac{d\theta_p}{d\varphi}$	$\frac{dV_{tw}}{d\varphi}$	$\frac{dV_{st}}{d\varphi}$	$\frac{dV_{sp}}{d\varphi}$
-90°	+0.0177	+6.846 × 10 <sup>-5</sup>	-0.374 × 10 <sup>-4</sup>	+2.950	-0.000 × 10 <sup>-4</sup>	+8.338 × 10 <sup>-4</sup>
-60°	+0.1617	+6.978 × "	-1.629 × "	+3.033	-2.239 × "	+2.258 × "
-30°	+0.2880	+4.281 × "	-2.463 × "	+1.867	-4.387 × "	-0.955 × "
0°	+0.3268	-0.095 × "	-2.698 × "	-0.063	-5.268 × "	-1.563 × "
+30°	+0.2578	-4.238 × "	-2.333 × "	-1.905	-4.412 × "	-2.044 × "
+60°	+0.1249	-6.526 × "	-1.461 × "	-2.937	-2.445 × "	-4.619 × "
+90°	-0.0051	-6.341 × "	-0.270 × "	-2.885	-0.363 × "	-9.380 × "

For part I :

$$\left. \begin{aligned} \frac{\theta}{p} &= 0.0001061 \cosh(1.78 s) \sin(1.78 s) + 0.0006084 \sinh(1.78 s) \cos(1.78 s), \\ \frac{V}{p} &= 0.3109 \sinh(1.78 s) \cos(1.78 s) - 1.783 \cosh(1.78 s) \sin(1.78 s), \\ \frac{1}{p} \frac{d\theta}{ds} &= 0.001275 \cosh(1.78 s) \cos(1.78 s) - 0.0008961 \sinh(1.78 s) \sin(1.78 s), \\ \frac{1}{p} \frac{dV}{ds} &= -2.626 \cosh(1.78 s) \cos(1.78 s) - 3.736 \sinh(1.78 s) \sin(1.78 s); \end{aligned} \right\} \quad (212)$$

and for part IV:

$$\left. \begin{aligned} \frac{\theta}{p} &= -0.00006922 \cosh(1.69 s) \sin(1.69 s) - 0.0006532 \sinh(1.69 s) \cos(1.69 s), \\ \frac{V}{p} &= 0.2149 \sinh(1.69 s) \cos(1.69 s) - 2.028 \cosh(1.69 s) \sin(1.69 s), \\ \frac{1}{p} \frac{d\theta}{ds} &= -0.001219 \cosh(1.69 s) \cos(1.69 s) + 0.0009852 \sinh(1.69 s) \sin(1.69 s), \\ \frac{1}{p} \frac{dV}{ds} &= -3.059 \cosh(1.69 s) \cos(1.69 s) - 3.784 \sinh(1.69 s) \sin(1.69 s). \end{aligned} \right\} \quad (213)$$

Table 26.

$\varphi$	$\frac{1}{p}\theta$	$\frac{1}{p}V_s$	$\frac{1}{p} \frac{d\theta}{d\varphi}$	$\frac{1}{p} \frac{dV_s}{d\varphi}$
-90°	+5.253 × 10 <sup>-4</sup>	-7.226 × 10 <sup>-3</sup>	-0.414 × 10 <sup>-4</sup>	-1.282 × 10 <sup>-3</sup>
-60°	+4.434 × "	-8.128 × "	-2.700 × "	-1.978 × "
-30°	+2.515 × "	-9.087 × "	-4.475 × "	-1.490 × "
0°	-0.046 × "	-9.548 × "	-5.043 × "	-0.178 × "
+30°	-2.537 × "	-9.284 × "	-4.236 × "	+1.106 × "
+60°	-4.314 × "	-8.530 × "	-2.440 × "	+1.613 × "
+90°	-5.037 × "	-7.773 × "	-0.314 × "	+1.127 × "

The required results of the calculations are shown in Table 27 and in Fig. 28~Fig. 31. In each of these figures, the length of the abscissa is taken as proportional to the length of the middle

layer in the meridian section of the pipe wall; and the positions of the sections corresponding to the "Section No." in the figures are given in Table 27.

Besides these results mentioned above, we must give the value of  $\delta$ , which is

$$\delta = 0.003589 t.$$

The deflection  $\Delta$  of the end of the tube under the pressure of 400 lbs. per sq. inch ( $28 kg/cm^2$ ) can be calculated easily by the values of  $\delta$ ,  $\omega_0$ ,  $r_0$  and  $\psi$ , and we have, in the present case,

$$\Delta = 0.592 cm \approx 6 mm,$$

which shows a close agreement with the actual deflection of the tube.

Table 27.

Section No.	$s$	$\varphi$	$\frac{1}{p}\sigma'_\varphi$	$\frac{1}{p}\sigma_{\varphi 0}$	$\frac{1}{p}\sigma''_\varphi$	$\frac{1}{p}\sigma'_\psi$	$\frac{1}{p}\sigma_{\psi 0}$	$\frac{1}{p}\sigma''_\psi$	$\frac{1}{p}\tau_m$	$\frac{1}{p} \cdot v \left[ \frac{cm^3}{kg} \right]$	$\frac{1}{p}(\eta - \delta) \left[ \frac{cm^3}{kg} \right]$
I	0	0	-61.87	+1.98	+65.83	-45.39	-19.54	+ 6.31	0.	0.	-3.223 × 10 <sup>-4</sup>
	1	$\frac{1}{4}l$	-58.44	+1.98	+62.40	-41.74	-16.92	+ 7.90	+0.82	-0.149 × 10 <sup>-5</sup>	-3.067 × "
	2	$\frac{1}{2}l$	-47.43	+1.98	+51.39	-30.89	- 9.38	+12.13	+1.81	-0.272 × "	-2.623 × "
	3	$\frac{3}{4}l$	-26.71	+1.98	+30.67	-13.16	+ 2.14	+17.44	+3.12	-0.335 × "	-1.943 × "
II	4	$l$	-90°	+ 6.93	+1.98	- 2.96	+10.58	+15.82	+20.99	+4.85	-0.321 × "
	5		-60°	+48.79	+4.70	-39.38	+29.03	+23.60	+18.17	+4.70	+1.349 × "
III	6		-30°	+82.74	+7.16	-68.41	+35.33	+17.89	+0.45	+2.98	+5.140 × "
	7		0°	+95.25	+8.12	-79.01	+29.00	+ 2.82	-23.36	+0.01	+6.947 × "
	8		+30°	+81.83	+7.05	-67.74	+15.47	-11.92	-39.31	-2.86	+5.353 × "
	9		+60°	+49.11	+4.68	-39.76	+ 2.56	-17.80	-38.16	-4.47	+1.763 × "
IV	10	$l$	+90°	+ 9.50	+2.10	- 5.30	- 4.15	-12.35	-20.55	-4.66	+0.068 × "
	11	$\frac{3}{4}l$		-21.37	+2.10	+25.57	- 0.98	+ 0.08	+ 1.14	-3.07	+0.119 × "
	12	$\frac{1}{2}l$		-40.88	+2.10	+45.08	+ 3.58	+10.50	+17.41	-1.83	+0.114 × "
	13	$\frac{1}{4}l$		-51.51	+2.10	+55.71	+ 7.21	+17.32	+27.43	-0.85	+0.068 × "
14	0		-54.87	+2.10	+59.07	+ 8.58	+19.69	+30.80	0.	0.	+3.240 × "

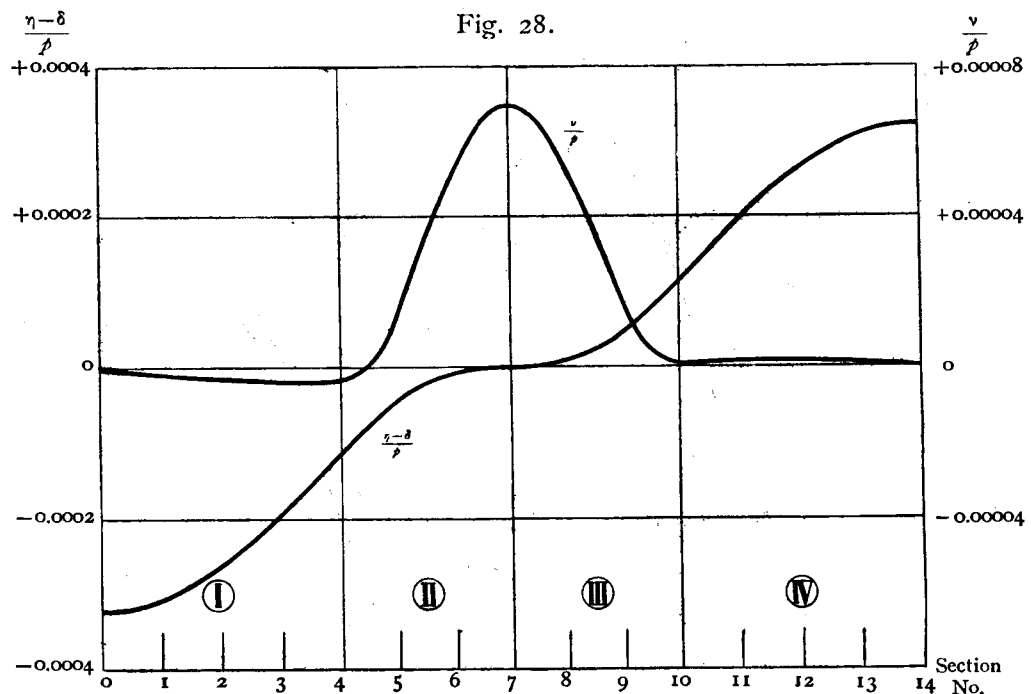


Fig. 29.

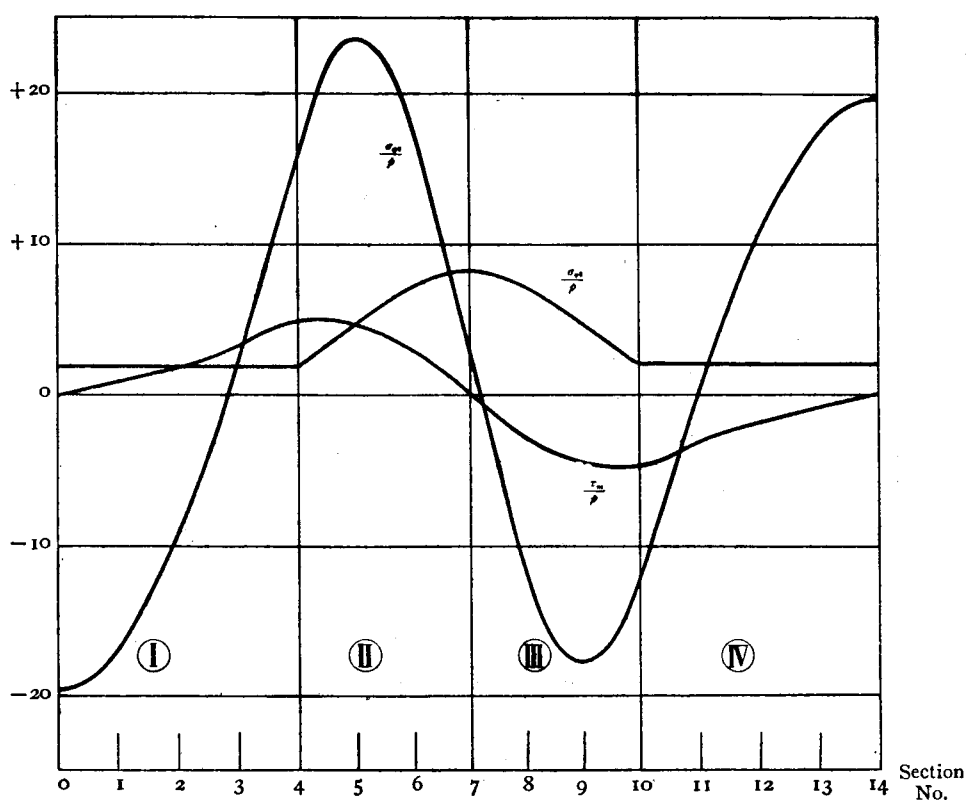


Fig. 30.

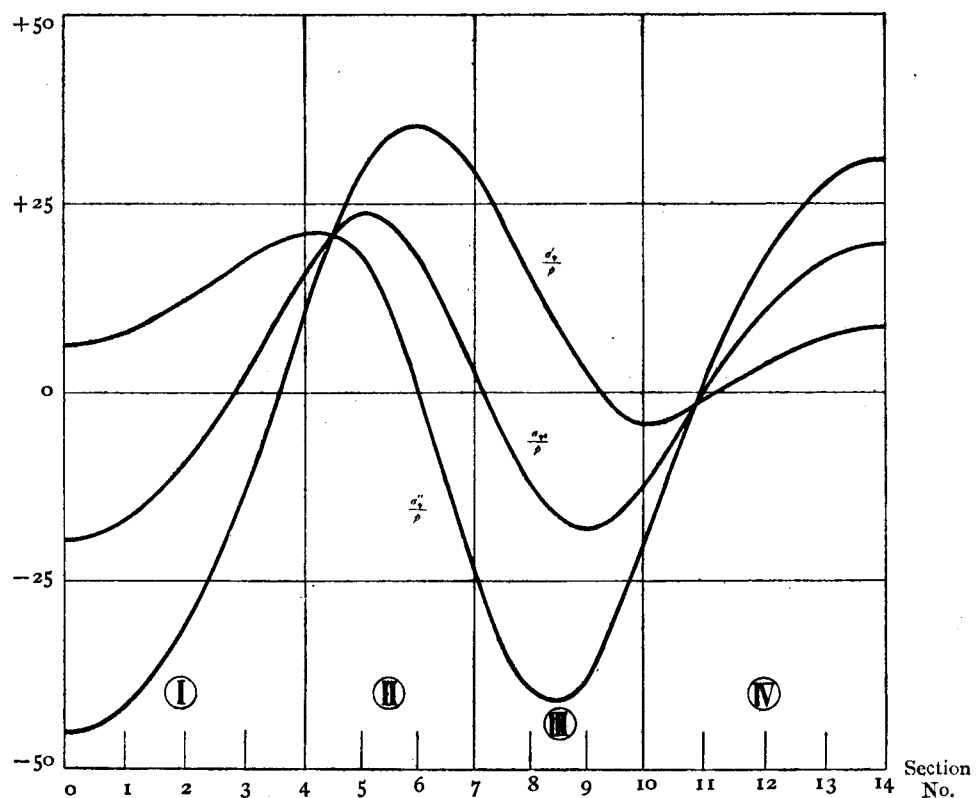
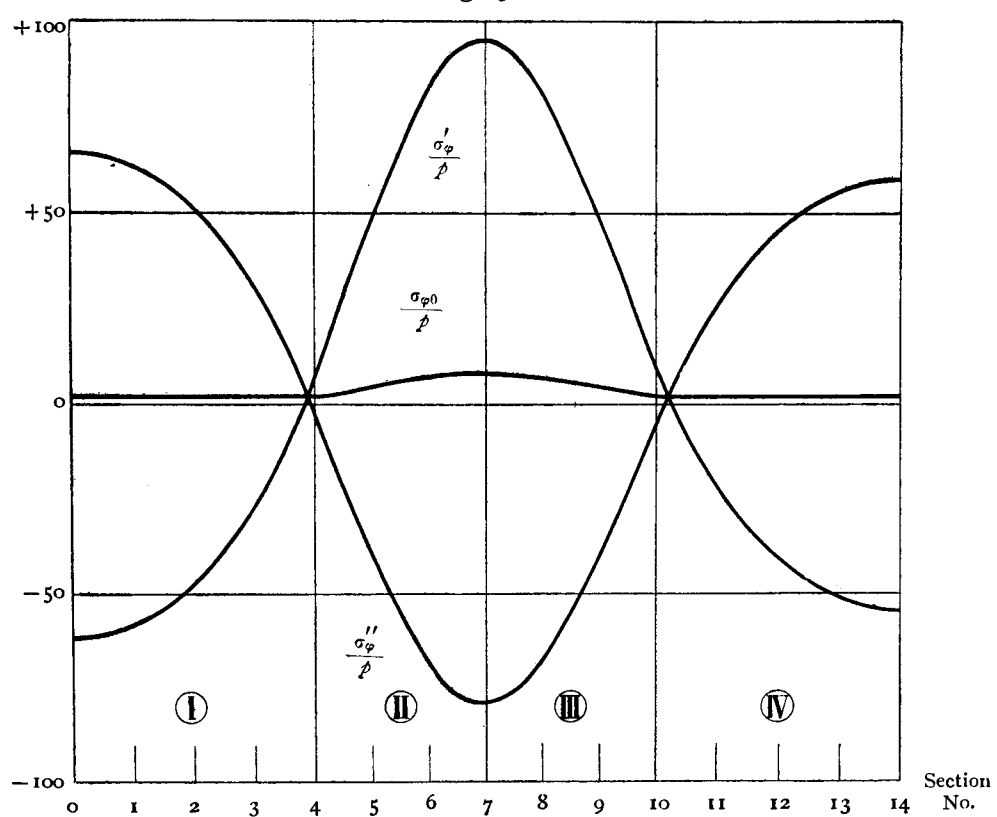


Fig. 31.



(Received Nov. 25, 1935)